Geochemistry Geophysics Geosystems G3
AN ELECTRONIC JOURNAL OF THE EARTH SCIENCES
Published by AGU and the Geochemical Society

Article
Volume 7, Number 4
18 April 2006
Q04010, doi:10.1029/2005GC001140
ISSN: 1525-2027

Submarine hydrothermal venting related to volcanism in the Lesser Antilles: Evidence from ferromanganese precipitates

M. Frank
Department of Earth Sciences, Institute for Isotope Geology and Mineral Resources, Eidgenössische Technische Hochschule Zürich, Eidgenössische Technische Hochschule Zentrum, F63, Sonneggstrasse 5, CH-8092 Zürich, Switzerland

Now at Leibniz-Institute for Marine Sciences, IFM-GEOMAR, Wischhofstrasse 1-3, 24148 Kiel, Germany (mfrank@ifm-geomar.de)

H. Marbler and A. Koschinsky
FB Geowissenschaften, Fachrichtung Geochemie, Hydrogeologie, Mineralogie, Freie Universitaet Berlin, Malteserstrasse 74-100, Haus B, D-12249 Berlin, Germany

Now at Geosciences and Astrophysics, School of Engineering and Science, International University Bremen IUB, P.O. Box 750561, D-28725 Bremen, Germany.

T. van de Flierdt
Department of Earth Sciences, Institute for Isotope Geology and Mineral Resources, Eidgenössische Technische Hochschule Zürich, Eidgenössische Technische Hochschule Zentrum, F63, Sonneggstrasse 5, CH-8092 Zürich, Switzerland

Now at Lamont Doherty Earth Observatory, Columbia University, 61 Rourte 9W, Palisades, New York 10964, USA

V. Klemm and M. Gutjahr
Department of Earth Sciences, Institute for Isotope Geology and Mineral Resources, Eidgenössische Technische Hochschule Zürich, Eidgenössische Technische Hochschule Zentrum, F63, Sonneggstrasse 5, CH-8092 Zürich, Switzerland

A. N. Halliday
Department of Earth Sciences, Institute for Isotope Geology and Mineral Resources, Eidgenössische Technische Hochschule Zürich, Eidgenössische Technische Hochschule Zentrum, F63, Sonneggstrasse 5, CH-8092 Zürich, Switzerland

Now at University of Oxford, Department of Earth Sciences, Parks Road, Oxford OX1 3PR, UK

P. W. Kubik
Paul Scherrer Institute, c/o Institute for Particle Physics, Eidgenössische Technische Hochschule Zürich, Eidgenössische Technische Hochschule, Hönggerberg, CH-8093 Zürich, Switzerland

P. Halbach
FB Geowissenschaften, Fachrichtung Geochemie, Hydrogeologie, Mineralogie, Freie Universitaet Berlin, Malteserstrasse 74-100, Haus B, D-12249 Berlin, Germany

[1] Radiogenic isotope compositions (Sr, Nd, Pb, Hf, and Os) of sediment-hosted seafloor ferromanganese crusts and sediments incrusted with ferromanganese oxyhydroxides from the Lesser Antilles island arc were measured to distinguish between hydrogenous (seawater-derived) and hydrothermal metal sources. The ages of the precipitates range between recent (last few thousand years) and a few 100 kyr as deduced from ^{10}Be and Co concentrations. Evidence from the presence of bladed todorokite and nontronite, together with the major element and REE composition, suggests that a significant proportion of these sediment-hosted precipitates formed at relatively low temperatures from a mixture of seawater and hydrothermal fluids associated with island arc volcanism. The radiogenic isotope compositions of all metals mentioned above, except Pb, show large differences in hydrothermal versus hydrogenous

contributions over space and time. In contrast to precipitates of high-temperature fluids which mainly scavenge their REE contents from seawater the crusts of this study show $^{143}Nd/^{144}Nd$ of up to 0.512817 ($\varepsilon Nd = +3.5$). This is close to the signature of the nearby island arc rocks and far above the expected local seawater ratio of ~0.51209 ($\varepsilon Nd = -10.7$). These crusts also show high $^{176}Hf/^{177}Hf$ (up to 0.283102), low $^{87}Sr/^{86}Sr$ (up to 0.7069), and low $^{187}Os/^{188}Os$ (up to 0.16) compared with local seawater, as expected from hydrothermal, island-arc-derived metal contributions. In contrast, the Pb isotope signatures of the crusts cannot be explained by mixing between seawater and hydrothermal sources. It is suggested that Pb was either removed from the ascending fluids within the sediment column before they reached seawater or the temperatures were too low to leach significant amounts of Pb from the rocks or sediments. External sources such as Saharan dust, particulate inputs from the Orinoco River, or even incongruent release of Pb isotopes from the island arc rock-derived particles must have contributed to the observed Pb isotope variability. Our results suggest that submarine hydrothermalism originating from intraoceanic island arc volcanism creates distinct geochemical environments for the dispersion of hydrothermal fluids and may be an important mechanism to supply metals of hydrothermal origin to seawater.

Components: 13,886 words, 9 figures, 5 tables.

Keywords: ferromanganese crusts; hydrothermal fluid; island arc volcanism; radiogenic isotopes; Lesser Antilles.

Index Terms: 1040 Geochemistry: Radiogenic isotope geochemistry; 1034 Geochemistry: Hydrothermal systems (0450, 3017, 3616, 4832, 8135, 8424); 1050 Geochemistry: Marine geochemistry (4835, 4845, 4850).

Received 9 September 2005; **Revised** 11 January 2006; **Accepted** 17 February 2006; **Published** 18 April 2006.

Frank, M., H. Marbler, A. Koschinsky, T. van de Flierdt, V. Klemm, M. Gutjahr, A. N. Halliday, P. W. Kubik, and P. Halbach (2006), Submarine hydrothermal venting related to volcanism in the Lesser Antilles: Evidence from ferromanganese precipitates, *Geochem. Geophys. Geosyst.*, *7*, Q04010, doi:10.1029/2005GC001140.

1. Introduction and Regional Setting

[2] Hydrothermal activity at mid ocean ridge (MOR) vent sites has been the focus of many geochemical and isotopic investigations since their initial discovery in 1977 (see summaries by *von Damm* [1995] and *Lowell et al.* [1995]). It has been shown that these high-temperature hydrothermal inputs play a significant role for the oceanic budgets of many dissolved metals in seawater (e.g., Sr, Os, Mn, etc.). Recently, it has been proposed that vent fields along intraoceanic arcs represent a potentially huge and previously unheeded source of fluids and metals to the ocean, which are different in composition from those originating at mid ocean ridges [*Gamo et al.*, 1997; *de Ronde et al.*, 2001, 2003; *Baker et al.*, 2005].

[3] The focus of this study is metal supply by submarine hydrothermal activity related to volcanism along the Lesser Antilles island arc stretching from northeastern Venezuela in the south to the Anegada Passage in the north. This passage is the tectonic boundary to the Greater Antilles (Puerto Rico–Virgin Islands platform). The Lesser Antilles arc is divided into a southern and a northern section, the latter represented by a double arc [*Fink*, 1972]. These two branches of the northern arc diverge north of Martinique (Figure 1). The northwestern branch (inner arc) consists of young volcanic islands including active volcanoes such as Soufrière Hills on Montserrat, and was probably initiated during the late Miocene. By contrast, the eastern branch represents much older tectonic activity [e.g., *Maury et al.*, 1990]. Submarine volcanic activity along the Lesser Antilles arc is well known and widespread [e.g., *Westercamp*, 1988; *Polyak et al.*, 1992; *Devine and Sigurdsson*, 1995] although little information is available on recent hydrothermal activity on the seafloor and hydrothermal mineral formation. Shallow hot springs were found offshore some islands including Dominica and Montserrat [*Johnson and Cronan*, 2001] but very little is known about occurrences in deeper waters [e.g., *Polyak et al.*, 1992]. To investigate hydrothermal activity, a research cruise with the R/V Sonne (SO-154) was carried out in January/February 2001, covering four different working areas between Montserrat and Grenada (Figure 1) [*Halbach et al.*, 2002]. Although no active hydrothermal vents were sampled, evidence for hydrothermal activity was detected in the water column and metal precipitates (ferromanganese crusts) of

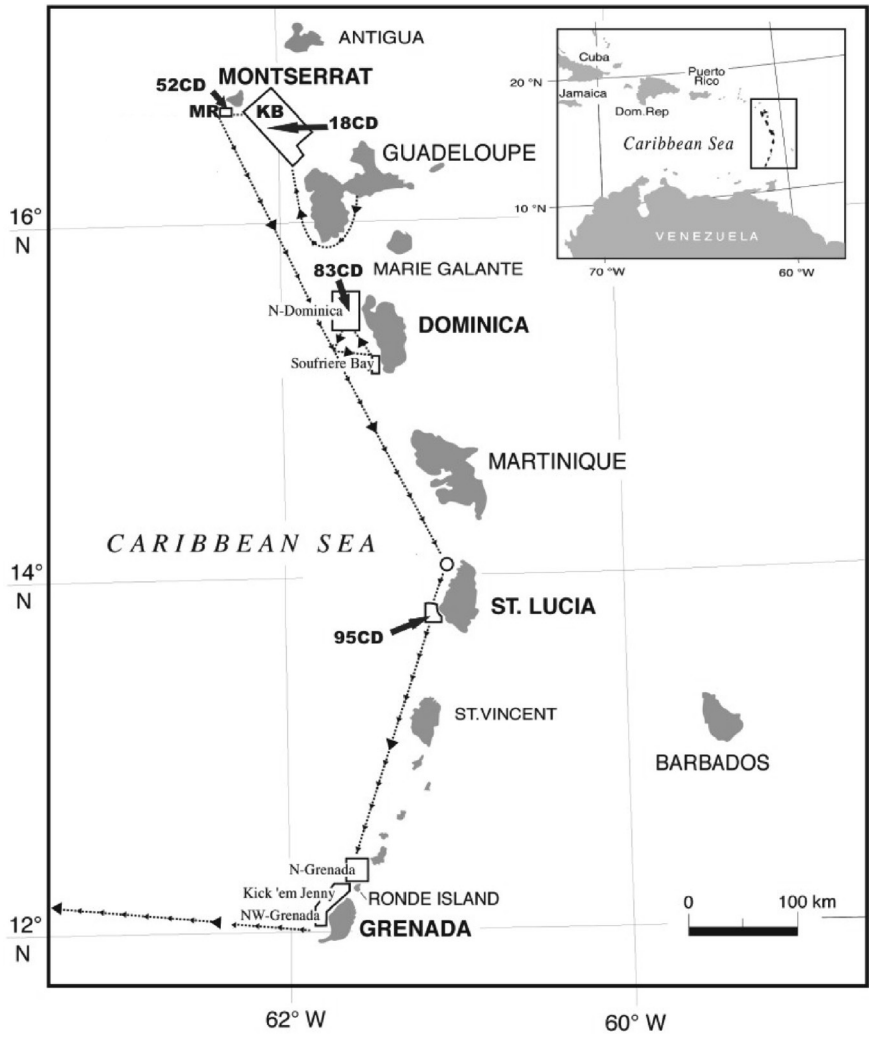

Figure 1. Map of the Lesser Antilles with cruise track (dashed line) and study areas (polygons) of RV *Sonne* cruise 154 in January/February 2001 as well as sample locations. KB, Kahouanne Basin; MR, Montserrat Ridge.

presumed hydrothermal origin as well as slightly hydrothermally altered rocks were collected. In the areas offshore the islands of Montserrat, Dominica and St. Lucia slightly increased CH_4 concentrations and reduced Cr(III) species were found [*Sander et al.*, 2003]. The strongest hydrothermal signals were measured close to the Kick'em Jenny submarine volcano northwest of Grenada, including high CH_4 and trace metal concentrations [*Koschinsky et al.*, 2002], although no hydrothermal precipitates were recovered at that location.

[4] In this study we focus on the use of radiogenic isotopes (Nd, Sr, Hf, Os, and Pb) as a tool to distinguish between seawater and hydrothermal origin of metals in ferromanganese crusts and sediments incrusted with ferromanganese oxyhydroxides. Radiogenic isotopes have been used successfully for this purpose [*van de Flierdt et al.*, 2004b] and other oceanographic and paleoceanographic applications in the past (see *Frank* [2002] for a recent review). The potential of radiogenic isotopes arises from the fact that weathering processes of different continental lithologies introduce distinct dissolved radiogenic isotope signatures to water masses, which are then advected and mixed as a function of the respective oceanic residence times of these metals. In contrast to these continental isotope signals in seawater, high-temperature hydrothermal fluids originating at MORs are characterized by a distinct radiogenic isotope signature reflecting the composition of the mantle. For some metals, such as Sr [*Palmer and Edmond*, 1989] and Os [e.g., *Peucker-Ehrenbrink and Ravizza*, 2000], these fluids contribute significantly to their seawater budget, whereas they are

Table 1. Locations of the Samples

Station	Location	Samples	Latitude	Longitude	Water Depth
18	Kahouane Basin	18CD	16°28.58–28.17′N	61°58.82–62°00.48′W	1144–987 m
52	Montserrat Ridge	52CD-X, 52CD-a	16°38.85–37.40′N	62°19.97–19.69′W	950–619 m
83	N.W. Dominica	83CD	15°32.51–32.79′N	61°34.44–33.74′W	1252–912 m
95	N.W. St. Lucia	95CD	14°00.50–00.49′N	61°05.06–04.44′W	1243–1059 m

not relevant for the budgets of others, such as REEs including Nd, that get immobilized very near the vent sites [*German et al.*, 1990; *Halliday et al.*, 1992]. Nothing is known as yet about the importance of hydrothermal fluids in intraoceanic back-arc systems for these metals, which is the subject of this study.

2. Material and Methods

[5] Lead, Nd, Hf, Os and Sr isotope compositions of different parts of 2 ferromanganese crusts together with 3 sediment samples incrusted with Mn and Fe oxide phases from different locations in the Lesser Antilles island arc were analyzed in this study. The samples were recovered during the Cruise SO-154 with R/V Sonne in January/February 2001 as part of the CARIBFLUX project. Sample locations are given in Figure 1 and Table 1. Massive crust 52CD-X was recovered by dredge on a large seamount, part of Montserrat Ridge near the island of Montserrat. Different macroscopically identifiable units are apparent in this crust, which were subsampled (Figure 2). The crust consists mostly of layers of ferromanganese oxyhydroxides (up to 2 mm thick) alternating with carbonate layers and patches of detrital material in a manganese-rich matrix in its outer parts. Redeposition of the carbonate and sandstone particles is apparent. Yellowish/green nontronite inclusions (up to 3 mm diameter) are common. The crust is overgrown by a thin, dark, massive, and essentially detritus-free ferromanganese crust of 1–2 mm thickness. A second massive crust (52CD-a) from the same location shows a mostly chaotic and much less pronounced layered structure of the same components as seen in crust 52CD-X. Two sandy to clayey hemipelagic sediment samples, which have been recovered nearby (51MC) and within the same dredge as the 52CD crusts are dominated by biogenic carbonates and contain abundant island-arc-derived rock fragments. No substrate rocks were recovered with either crust but there is clear evidence from the partly cemented sediments that were recovered by the same dredge that the crusts precipitated on the sediment cover of Montserrat Ridge. One sediment sample with ferromanganese matrix (18CD) from the Kahouanne Basin south of the island of Montserrat was analyzed. Samples 83CD and 95CD-1 represent ferromanganese precipitates on sediments from a seamount north of Dominica and from a seamount north of St. Lucia, respectively. These precipitates occur as flat slabs on the surface of the sediments or as strata-bound layers within the sediments. They are coarsely layered with a botryoidal porous texture of up to 1.5 cm thickness on top of the sediments. The strata-bound layers are up to 8 cm thick.

[6] Nine subsamples of crust 52CD-X representing the macroscopically different layers and 5 subsamples of 52CD-a were analyzed (Figure 2). Between 50 and 500 mg of these samples and the three encrusted sediments were leached in 6 M HCl for ~15 min (for Hf isotope analyses they were leached with a mixture of 6M HCl and a few drops of concentrated HF). Residual material (less than 10% of the total weight of the samples) was removed by centrifugation. Chemical separation and purification followed standard procedures for Nd [*Cohen et al.*, 1988], Pb [*Lugmaier and Galer*, 1992], Hf [*Lee et al.*, 1999], and Sr [*Horwitz et al.*, 1992]. Because of the relatively high amounts of carbonate, Sr isotope analyses were carried out on an additional set of aliquot samples, which were leached with 10% acetic acid and rinsed thoroughly prior to leaching and dissolution of the Mn-Fe oxides and oxyhydroxides in 6M HCl. All above radiogenic isotope compositions were measured on a Nu Instruments multiple collector inductively coupled plasma mass spectrometer (MC-ICPMS). The Pb isotopes were measured applying a Tl-doping procedure [e.g., *Belshaw et al.*, 1998]. Measured $^{143}Nd/^{144}Nd$, $^{87}Sr/^{86}Sr$ (corrected for Kr interferences) and $^{176}Hf/^{177}Hf$ were normalized to $^{146}Nd/^{144}Nd = 0.7219$, to $^{88}Sr/^{86}Sr = 8.3752$ and to $^{179}Hf/^{177}Hf = 0.7325$, respectively, to correct for instrumental mass bias. All radiogenic isotope ratios presented are normalized to given standard values: For JMC-Nd, a given $^{143}Nd/^{144}Nd$ value of 0.511833, cross calibrated to the La Jolla standard (0.511858); for NIST SRM981 the Pb isotope

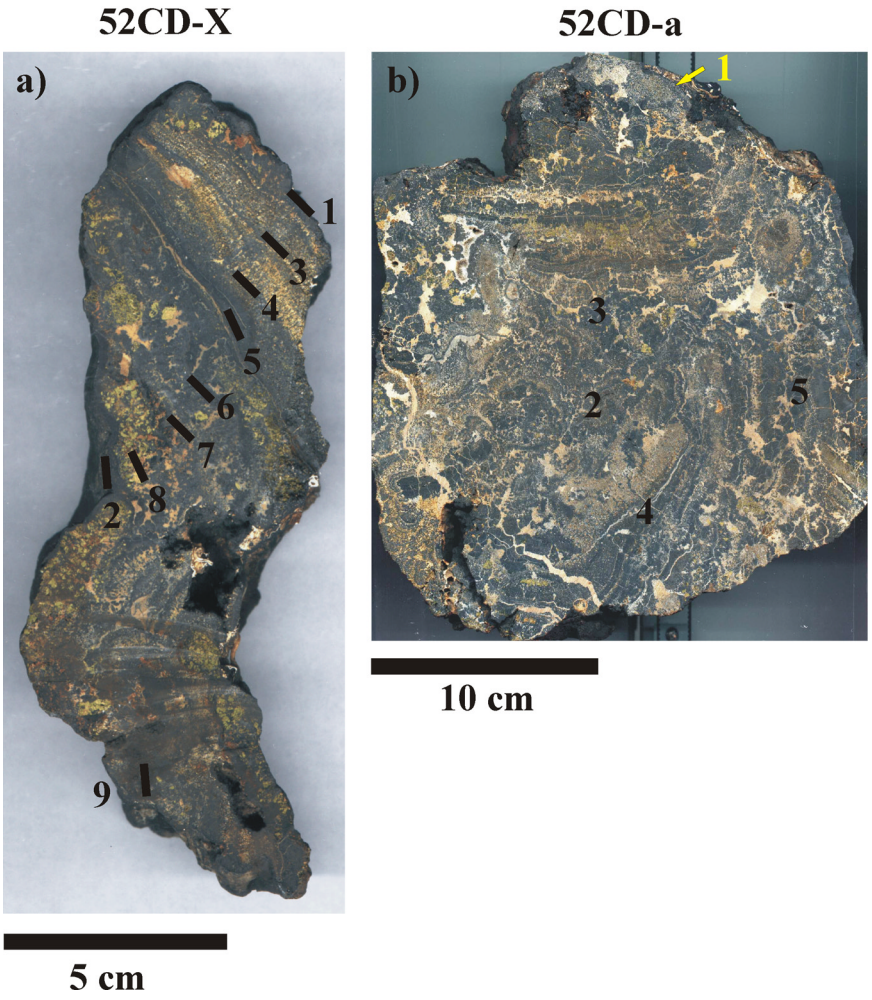

Figure 2. Photographs of (a) crust 52CD-X and (b) crust 52CD-a. The sampled sections are marked by numbers, which correspond to the sample numbers in the tables and the text. Despite the fact that there is no clearly defined top or bottom we define sample 1 as being at the top.

ratios by *Galer and Abouchami* [1998]; for NIST SRM987, a given $^{87}Sr/^{86}Sr$ value of 0.710245; and for JMC475 a given $^{176}Hf/^{177}Hf$ of 0.282160 were used for external normalization. The 2σ external reproducibility for the $^{143}Nd/^{144}Nd$ measurements varied between 35 and 51 ppm; for $^{206}Pb/^{204}Pb$, $^{207}Pb/^{204}Pb$, and $^{208}Pb/^{204}Pb$ it varied between 180 and 250 ppm, for $^{207}Pb/^{206}Pb$ it was 65 ppm, and for $^{208}Pb/^{206}Pb$ it was 115 ppm; for $^{87}Sr/^{86}Sr$ measurements it varied between 36 and 38 ppm, and for $^{176}Hf/^{177}Hf$ measurements it varied between 42 and 45 ppm. In-run precision for each sample was better than the external reproducibility, with the exception of a few low-concentration Pb isotope measurements. The Nd isotope measurements were disturbed by a matrix effect, most probably caused by the presence of Ba (up to 10V beam intensity on mass 138), which was mirrored by significant deviations of the measured $^{145}Nd/^{144}Nd$ in the same samples from the primordial ratio, as obtained by the standard measurements. Dilution of the sample solutions reduced the effect significantly for most samples. Only those Nd isotope results, for which the $^{145}Nd/^{144}Nd$ ratio was within 2σ of the ratio measured for the standard, were accepted.

[7] Osmium isotope compositions and concentrations were measured on 9 subsamples of crust 52CD-X from the same horizons as for the other isotopes, but not on aliquot samples. Two aliquot subsamples of 52CD-a and one each of 83CD, 95CD and 18CD were also analyzed for Os isotopes. Each sample, weighing between 20 and 150 mg, was leached in double distilled, concentrated HBr for ~15 min and any residual material was removed by centrifuging to avoid leaching of detrital material during the standard chemistry

procedure [*Birck et al.*, 1997; *Klemm et al.*, 2005]. Samples were then measured by negative thermal ionization mass spectrometry (N-TIMS) closely following published methods [e.g., *Creaser et al.*, 1991; *Volkening et al.*, 1991; *Birck et al.*, 1997]. The total procedural blank for Os during this study was 0.32 ± 0.01 pg/g resulting in a blank correction not greater than 1%. The external reproducibility of the Os isotope measurements was similar to the internal precision of the individual measurements.

[8] It is noted here that the differences in leaching solutions and leaching techniques applied for Nd and Sr in comparison with those applied for Hf and Os are not expected to introduce any significant bias from potentially variable leaching of these elements from incorporated detrital material. As mentioned above, the amount of detrital particles is low and the concentrations of the elements of interest within the detrital particles (mostly island arc rocks) are low in comparison with those in the ferromanganese oxyhydroxides. The removal of the carbonate fraction with dilute acetic acid prior to Sr isotope analysis is also not expected to cause any bias because carbonates contain only very low amounts of the metals studied here and acetic acid does not attack the ferromanganese oxyhydroxides. Therefore the isotopic and elemental compositions of the leached fractions are considered to be comparable for each sample.

[9] For the subsamples of crust 52CD-X we also performed analyses of ^{10}Be (following the chemical purification procedure given by *Henken-Mellies et al.* [1990]) and ^{9}Be concentrations to investigate if the layering corresponds to an age distribution. The samples of this study were measured at the Zürich AMS facility of the Paul Scherrer Institute and the ETH Zürich, Switzerland. The ^{10}Be concentrations were normalized to internal standard S555 with a nominal ^{10}Be/^{9}Be value of 95.5×10^{-12}. The 1σ statistical uncertainties of individual ^{10}Be measurements take into account both the counting statistics of the ^{10}Be "events" and the reproducibility of repeated measurements, which were performed on each sample. The concentrations of ^{9}Be along with ^{59}Co were measured by ICP-MS at the Laboratory of Inorganic Chemistry, ETH Zürich, using an ELAN 6100 DRC ICP-MS instrument, on aliquots of the same samples used for ^{10}Be analyses. Direct analysis of pressed powder pellets of the Nod A-1 ferromanganese crust standard by laser ablation ICP-MS [*Günther et al.*, 2000] at the Laboratory of Inorganic Chemistry reproduced the published data of *Axelsson et al.* [2002]. However, the data obtained by solution nebulization were offset by a constant amount. The reason for this discrepancy is unclear but a matrix effect is the most likely explanation. To correct for this, all solution measurements were normalized by comparing the measured and accepted values for Nod A-1 [*Axelsson et al.*, 2002]. Following complete dissolution of a separate sample set, additional analyses for major and minor element concentrations were performed by AAS and ICP-AES at the Free University (FU) Berlin. Analyses of REEs and other low-concentration elements were carried out by ICP-MS at the National Oceanography Centre (NOC), United Kingdom. The mineralogical composition of the precipitates was analyzed using X-Ray diffraction (XRD) and Scanning Electron Microscope (SEM) techniques at the FU Berlin. The two sediment samples (51MC and 52CD) were subjected to a weak leach in an oxalate cocktail at room temperature [*Tovar-Sanchez et al.*, 2003], which was originally developed to extract iron under trace metal clean conditions from phytoplankton. This procedure was expected to release trace metals from the sediments, either originally adsorbed to dust particles or scavenged from seawater. The remaining fractions were then leached with 6 M HCl, the residue was finally completely dissolved and all fractions were analyzed for their Nd, Pb, Sr, and Hf isotope composition.

3. Results

3.1. Mineralogical and Element Geochemical Evidence for Hydrothermal Origin

[10] Mineralogical composition of the samples, as determined by X-ray diffraction (XRD), microscopy and SEM show that the layered parts of the massive crusts are dominated by todorokite (10 Å manganite), whereas the 2 mm thin layer that overgrew the entire sample 52CD-X consists of δMnO_2 and FeOOH (vernadite). The ferromanganese matrix of the 3 sediment samples consists mainly of vernadite and todorokite. The presence of massive todorokite and rhythmically precipitated, bladed todorokite in the inner parts of the two massive crusts provides clear evidence that they precipitated from a mixture of relatively low temperature hydrothermal fluid and seawater [*Usui et al.*, 1988; *Percival and Ames*, 1993]. Nontronite, a hydrous Fe-Na phyllosilicate of hydrothermal origin, did not coprecipitate together with the ferro-

Table 2. Concentrations of Selected Major and Minor Elements for Different Types of Lesser Antilles Crusts and Incrustations of Sediments[a]

	Sample									
	52CD-x1	52CD-x3	52CD-x4	52CD-a1	52CD-a2	52CD-a4	52CD-a5	18CD	83CD	95CD
Description	surface of massive crust	inner layer of massive crust	inner layer of massive crust	outer layer of massive crust	inner layer of massive crust	inner layer of massive crust	inner layer of massive crust	stratabound Mn layer in sediment	Mn-incrustation on sediment	Mn-incrustation on sediment
Mn, wt.%	22.00	44.03	38.32	23.00	45.26	45.48	45.10	33.25	19.26	26.93
Fe, wt.%	18.20	1.31	0.86	9.01	0.52	0.52	0.71	4.71	7.34	9.99
Mn/Fe	1.21	33.70	44.59	2.55	87.27	88.10	63.10	7.05	2.63	2.70
Al_2O_3, wt.%	1.89	1.26	1.68	2.44	1.02	1.23	1.98	5.76	8.30	7.09
MgO,[b] wt.%	2.57	3.11	2.94	3.23	327	3.55	3.42	1.58	3.95	4.64
CaO,[b] wt.%	4.61	5.25	3.97	7.67	6.28	5.1	6.7	2.15	6.07	1.4
P, ppm	2738	397	655	5433	589	632	625	408	1030	1410
Co, ppm	2400	20	20	236	82	32	42	335	60	158
Zn, ppm	760	149	311	266	147	101	111	587	246	691
Ni, ppm	3935	225	470	512	123	121	141	1279	460	790
Li, ppm	86	131	160	63	59	61	83	101	252	494
Pb, ppm	1247	10	7	75	3	2	11	52	8	51
Ba, ppm	3160	3390	2900	919	2530	3130	4360	599	906	775
Ti, ppm	521	648	392	6670	322	266	457	864	1830	1330
Sr, ppm	1059	911	834	758	1460	1750	3100	710	1440	482

[a] Data were analyzed by ICP-AES and XRF.
[b] These samples include the carbonate fraction, which was removed prior to measurement of the other elements and the Sr isotopes.

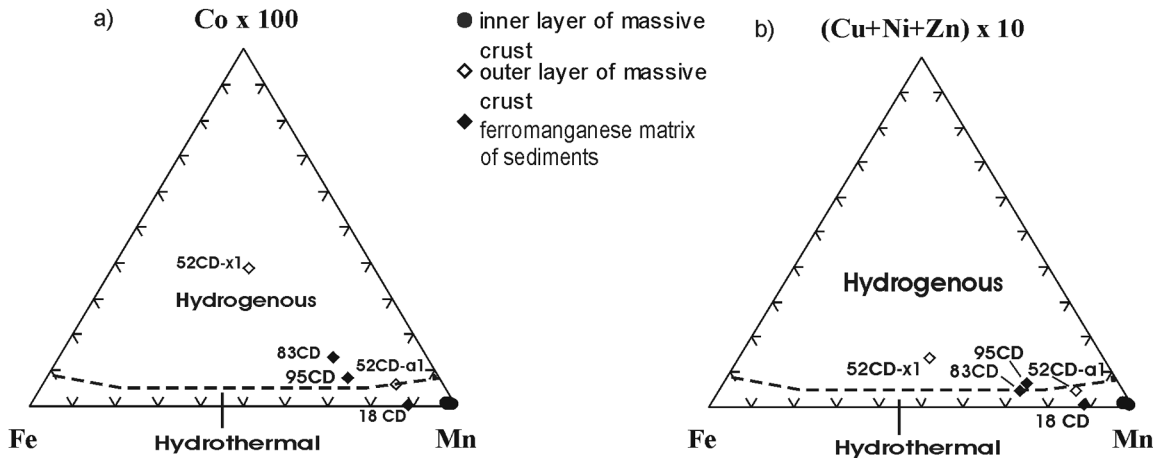

Figure 3. Ternary diagram of the concentration of Mn and Fe in the two crusts and the ferromanganese matrix of the sediment samples with (a) hundredfold concentration of Co and (b) tenfold concentration of Ni + Cu + Zn. The hydrothermal and hydrogenous fields are taken from *Usui and Nishimura* [1992].

manganese oxyhydroxides but was redeposited from immediately nearby sources. It is abundant in the inner parts of these crusts and clearly indicates hydrothermal activity. Dominating vernadite in the outer thin layers of the massive crusts as well as in the ferromanganese matrix of the sediment samples suggests that these were dominated by metals supplied directly from seawater [*Usui et al.*, 1988].

[11] The concentrations of selected major and minor elements in different parts of the precipitates show a large variability (Table 2). The element composition of the outer layer of crust 52CD-X (sample 52CD-x1) and incrusted sediments 83CD and 95CD is similar to hydrogenetic ferromanganese crusts (Figure 3) [e.g., *Usui and Nishimura*, 1992; *Frank et al.*, 1999]. The inner parts of the two massive crusts are characterized by high Mn/Fe values of up to 88 together with very low concentrations of other trace metals generally enriched in hydrogenetic crusts, such as Co, Pb, or Ni [e.g., *Frank et al.*, 1999]. This composition is consistent with both high growth rates and concentrations observed in modern hydrothermal crusts [*Hein et al.*, 1997]. The ferromanganese matrix of the sediments and the surface of the other massive crust (52CD-a) are intermediate between the above described hydrogenetic and hydrothermally influenced compositions, consistent with the evidence from the mineralogical composition described above (Figure 3). Further corroboration of a largely hydrothermal origin comes from ternary plots of Mn and Fe contents versus those of Ni, Co, Cu, and Zn (Figure 3) [*Usui and Nishimura*, 1992] with all the internal parts of the two massive crusts plotting in the Mn-rich part of the hydrothermal fields of these diagrams. As described in the methods section above, these results have been obtained from element concentrations after complete dissolution of the samples. The hydrothermal signatures would thus even be more pronounced if the same elements had been measured on leachates of these samples.

[12] The REE data (Table 3) show a large variability between the different types of precipitates. Consistent with the concentrations of the other trace metals (Co, Ni, Zn, Pb) the inner hydrothermal layers of the massive crusts represent the low end of the range of REE concentrations, whereas the matrix of the sediment samples and the outer hydrogenetic layers of the crusts plot at the high end. The shale (PAAS)-normalized REE patterns are shown in Figure 4 and are relatively flat which may indicate a detrital sediment contribution. Nevertheless all the hydrothermal samples show moderate HREE enrichments (e.g., low Nd_n/Yb_n values between 0.26 and 0.75 and La_n/Yb_n values between 0.29 and 0.73), which, together with low trace element concentrations have been interpreted as indicative of low-temperature fluids [e.g., *Hodkinson et al.*, 1994; *Mills et al.*, 2001]. For comparison, high-temperature hydrothermal deposits have Nd_n/Yb_n values significantly above 1 and are thus clearly distinct [e.g., *Mills and Elderfield*, 1995; *Rimskaya-Korsakova and Dubinin*, 2003]. There are also distinct differences in the PAAS-normalized REE patterns with the outer (hydrogenetic) layers of the crusts and the matrix of sediment samples 18CD and 95CD all showing positive Ce_n anomalies, similar to other

Table 3. Rare Earth Element Content of Various Crust Types

Element, ppm	52CD-x1	52CD-x3	52CD-x4	52CD-a1	52CD-a2	52CD-a4	18CD	83CD-1	95CD-1
La	354.74	4.08	6.47	11.40	1.79	4.72	21.87	10.09	32.02
Ce	1343.8	4.10	7.31	38.36	2.70	7.27	63.31	17.50	73.38
Pr	77.01	0.73	1.33	2.42	0.38	0.92	4.83	2.04	6.93
Nd	332.61	3.21	5.83	10.42	1.66	3.97	20.57	8.55	28.25
Sm	71.28	0.72	1.30	2.41	0.41	0.96	4.62	1.93	6.24
Eu	17.44	0.13	0.31	0.64	0.06	0.20	1.24	0.44	1.56
Gd	105.23	0.91	1.56	2.73	0.45	1.15	5.60	2.18	6.37
Tb	14.34	0.14	0.24	0.43	0.07	0.17	0.90	0.35	1.00
Dy	81.18	0.99	1.57	2.71	0.50	1.18	5.68	2.39	6.13
Ho	16.61	0.23	0.36	0.58	0.11	0.27	1.23	0.52	1.23
Er	44.86	0.68	1.11	1.64	0.34	0.77	3.63	1.51	3.26
Tm	6.94	0.11	0.17	0.25	0.05	0.11	0.57	0.24	0.48
Yb	45.88	0.68	1.04	1.59	0.31	0.69	3.51	1.45	2.80
Lu	6.69	0.11	0.17	0.23	0.05	0.10	0.54	0.23	0.40

hydrogenetic crusts and nodules [e.g., *Elderfield et al.*, 1981; *Koschinsky et al.*, 1997; *Kuhn et al.*, 1998]. By contrast, the inner layers of the massive crusts show negative Ce_n anomalies and small negative Eu_n anomalies, typical of relatively low-temperature hydrothermal precipitates [e.g., *Kuhn et al.*, 1998; *Mills et al.*, 2001]. In particular, the negative Eu_n anomalies indicate nondissolution of plagioclase and thus temperatures below 220°C of the hydrothermal fluids during the fluid/rock interaction within the seafloor [*Douville et al.*, 1999; *Zierenberg et al.*, 1995]. These results thus do not only provide evidence for low temperatures during precipitation of the crusts, which may have been a consequence of cooling of initially high-temperature fluids during ascent through the sediments above the vent sites, but also for initially low temperatures prior to entering the sediments. These patterns essentially exclude that the REEs and also the signatures of the radiogenic isotopes presented in this study (except Pb) have been influenced significantly by attacking detrital particles within the crusts in the course of our leaching procedures. The detrital particles in the crusts mainly originate from the volcanic island arc rocks which generally show a slightly positive Ce_n anomaly and a strongly positive Eu_n anomaly.

[13] In summary, the above mineralogical and geochemical evidence suggests that the interior

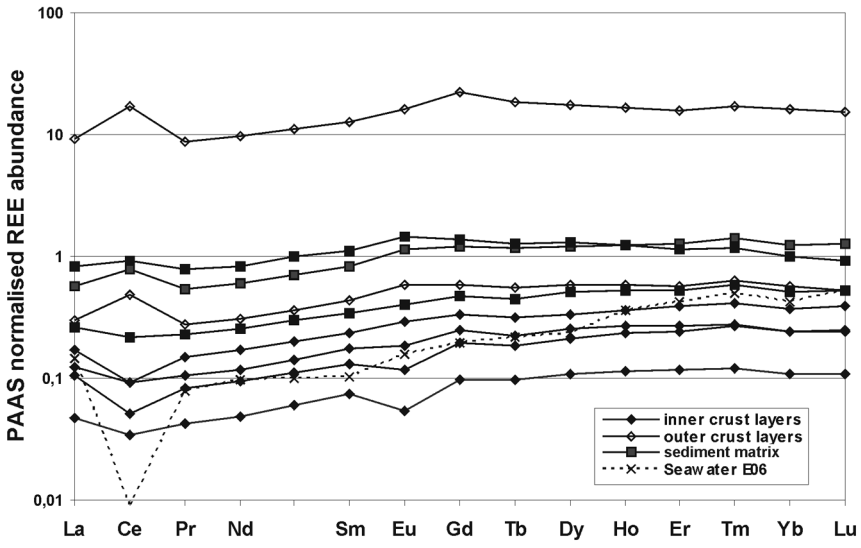

Figure 4. Post Archaean Average Sedimentary rocks (PAAS) [*McLennan*, 1989] normalized REE patterns for the crusts and the ferromanganese matrix of the sediment samples together with the pattern($\times 10^6$) for Atlantic seawater [*German et al.*, 1990]. Nonnormalized REE concentrations are given in Table 3.

Table 4. Be Isotope Results for Crust 52CD-x

Sample	Depth, mm	^{10}Be ± 1σSE, × 10^8 atoms/g	^{9}Be$_{meas.}$, ppm	^{9}Be$_{corr.}$, ppm	^{10}Be/^{9}Be ± 1σSE, × 10^{-8}	^{10}Be, Ma	^{10}Be/^{9}Be, Ma
1	0–1	189.07 ± 6.69	3.4	4.9	5.727 ± 0.608	0.0 ± 0.0	0 ± 0
2	0–2	282.49 ± 16.19	7.2	10.6	4.005 ± 0.462		0.78 ± 0.09
3	6–8	6.37 ± 0.39	0.8	1.2	0.793 ± 0.093	7.4 ± 0.5	4.34 ± 0.51
4	17–19	1.46 ± 0.18	0.4	0.6	0.373 ± 0.059	10.7 ± 1.3	5.99 ± 0.95
5	23–24	0.88 ± 0.18	0.2	0.3	0.465 ± 0.106	11.8 ± 2.4	5.50 ± 1.25
6	35–36	1.79 ± 0.20	0.2	0.3	0.784 ± 0.118	10.2 ± 1.1	4.36 ± 0.66
7	44–47	1.51 ± 0.14	0.3	0.4	0.535 ± 0.073	10.6 ± 1.0	5.20 ± 0.71
8	61–67	9.71 ± 0.59	1.3	2.0	0.740 ± 0.087	6.5 ± 0.4	4.49 ± 0.53
9	69–70	14.15 ± 0.78	1.1	1.6	1.363 ± 0.156	5.7 ± 0.3	3.15 ± 0.36

parts of the massive crusts grew from a mixture of seawater and low-temperature hydrothermal fluids, which, after cessation of the hydrothermal fluid supply, were overgrown by a thin layer of hydrogenetic ferromanganese crust.

3.2. ^{10}Be Concentrations and ^{10}Be/^{9}Be

[14] In order to gain information on the origin and possibly the growth rate of the crusts as well as the duration of hydrothermal activity, a profile of 9 measurements (Figure 2) of ^{10}Be and ^{9}Be concentrations through crust CD52-X was obtained (Table 4 and Figure 5). The ^{10}Be concentrations of the two surface samples taken from two different places of the crust are similar to other hydrogenetic crusts [e.g., *van de Flierdt et al.*, 2003, 2004a; *Frank et al.*, 2003]. The ^{10}Be/^{9}Be values at the surface (5.7 and 4.0 × 10^{-8}; samples 1 and 2 in Figure 2, respectively) are similar to values for north Atlantic seawater at about 1000 m depth [*Ku et al.*, 1990] and are essentially within the range between 0.39 and 0.5 × 10^{-8} obtained for surfaces of other deep Atlantic hydrogenetic ferromanga-

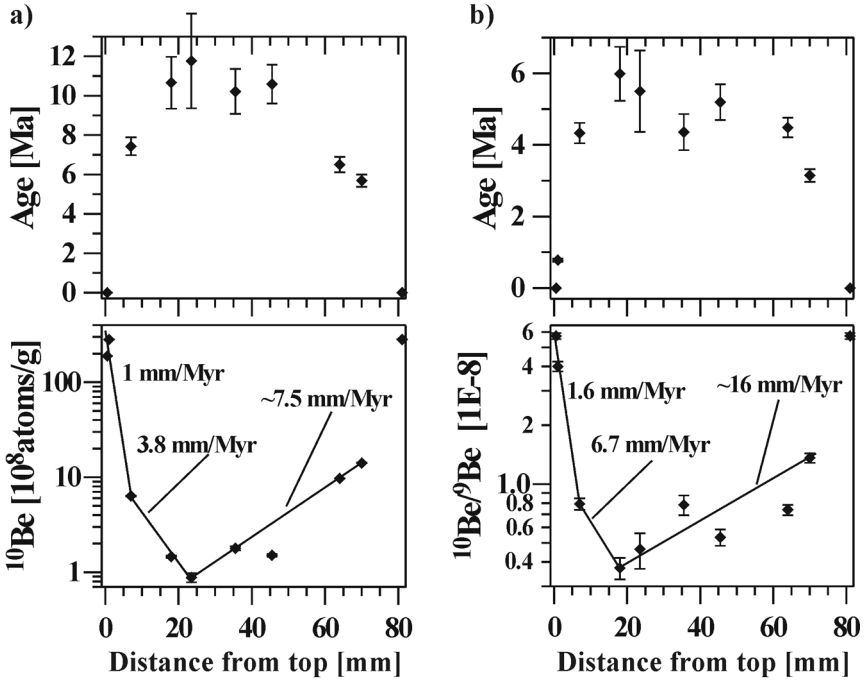

Figure 5. Profiles of (a) ^{10}Be concentrations and (b) ^{10}Be/^{9}Be values together with the corresponding ages in million years (Ma) versus distance from the top surface of crust 52CD-X (Figure 2). The ages have been calculated with a half-life for ^{10}Be of 1.5 Myr and assuming constant initial ^{10}Be concentrations and ^{10}Be/^{9}Be ratio. They represent maximum estimates, which are most likely not realistic (see text). The surface values are plotted again at a depth of 80 mm to indicate that the hydrothermal part of the crust has been overgrown by a thin layer of hydrogenetic crust. The growth rates in mm/Myr have been calculated from best fits to the data.

nese crusts [*von Blanckenburg et al.*, 1996a]. This demonstrates that the thin hydrogenetic surface layer represents the present-day growth surface. The ^{10}Be concentrations in this layer suggest typical hydrogenetic growth rates on the order of 1 to 5 mm/Myr resulting in an age of the surface layer on the order of a few 100 kyr.

[15] To the interior of the hydrogenetic surface layer, ^{10}Be concentrations and ^{10}Be/^{9}Be values decrease rapidly. Given that the decrease in ^{10}Be concentration (by a maximum factor of ~200) was mainly caused by dilution with the rapidly accumulating metals of hydrothermal origin in the interior part of the crust, the resulting maximum age of 11.8 ± 2.5 Ma at 23 mm depth of the crust is not realistic (Figure 5). Considering likely hydrothermal contributions of ^{9}Be [*Bourlès et al.*, 1991, 1994; *Seyfried et al.*, 2003], it is also not possible to reliably interpret the low ^{10}Be/^{9}Be values in the inner section of crust CD52-X in terms of age (6 ± 1 million years; Figure 5). This is supported by evidence from growth rate estimations for the inner parts of the crust based on Co-constant flux modeling. Translation of the measured Co concentrations into growth rates following the approach of *Manheim* [1986] results in values up to several 1000 mm/Myr. This does not even take into account that some of the Co may have been supplied by hydrothermal sources as well. Together with the evidence from the occurrence of radially growing todorokite crystals and gel-like structures in the inner parts of the crust, which also suggest rapid growth, this indicates that the ^{10}Be/^{9}Be values were entirely dominated by varying and unquantifiable hydrothermal contributions of ^{9}Be.

[16] In summary, this means that the hydrothermally influenced inner part of the crust grew fast over a period of hydrothermal activity of at maximum a few 10,000 years duration. Hydrothermal activity ceased not longer than a few 100 kyr ago, which is confined by the period of time represented by the hydrogenetic surface layer.

3.3. Radiogenic Isotopes

[17] The results of the Nd, Hf, Pb, Os and Sr isotope analyses are listed in Table 5 and plotted in Figures 6–9. Large variations between samples and within the massive crusts were found for all these analyses.

[18] In crust 52CD-X, the Nd isotope composition ranges from ε_{Nd} of −10.7 in the hydrogenetic surface layer to ε_{Nd} of +3.5 at 18 mm distance from the outer layer (sample 4 in Figure 2; see also Figure 6), which corresponds to the highest hydrothermal contribution of ^{9}Be, as derived from the minimum in ^{10}Be/^{9}Be (Figure 5). Hydrogenetic crusts incorporate and preserve the radiogenic isotope composition of ambient deep water (see *Frank* [2002] for a recent review). The low ε_{Nd} values of the hydrogenetic surface layer of 52CD-X as well as of CD52-a are thus considered representative of seawater at this location. This is supported by unpublished ε_{Nd} data between −11.0 and −11.5 obtained for a hydrogenetic ferromanganese crust from 2000 m water depth in the deep central Caribbean Sea [*Whiteley*, 2000]. The surface ε_{Nd} value of 52CD-X is also within error identical to a value of −10.9, which was obtained for the surface of hydrogenetic crust BM1963.897 from a depth of 800 m at the Blake Plateau [*Reynolds et al.*, 1999], which is today, at this depth, bathed in waters from the Caribbean. All higher ε_{Nd} values represent a mixture between Nd derived from seawater and hydrothermal fluids, which are expected to have either mantle-like ε_{Nd} values on the order of +10 or values similar to the composition of neighboring island arc rocks (between +2 and +10). The interior of crust 52CD-a also shows ε_{Nd} values higher than seawater but does not reach the maxima of 52CD-X. Of the sediments with ferromanganese matrix only sample 83CD shows a sizable deviation from the ambient seawater value. The variations in isotope composition correlate inversely with Nd concentrations in 52CD-X, which are higher by up to a factor of 150 in the hydrogenetic surface layer of the crusts than in the inner parts (Figure 7).

[19] We observe a similar but somewhat more complicated pattern of variability in the Sr, Hf and Os isotope compositions of the two crusts (Figure 6). The hydrogenetic surface of 52CD-X is within error identical to modern seawater (^{87}Sr/^{86}Sr = 0.709163 ± 25) consistent with the surface layer being a pristine seawater precipitate. All samples from the interior of this crust have lower ^{87}Sr/^{86}Sr, with the lowest measured ratio in the carbonate-free Mn-Fe oxyhydroxide fraction being equal to 0.706912 and corresponding to the same sample as the highest Nd isotope ratio (Figures 6, 7, and 8). Lower values are also explainable by mixing with hydrothermally supplied Sr, which has ^{87}Sr/^{86}Sr as low as 0.7035 in mantle-derived rocks and in the nearby island arc rocks. In contrast to the variable Sr isotopes in crust 52CD-X, analyses of crust 52CD-a and the

Table 5 (Representative Sample). Radiogenic Isotope Compositions and Concentrations [The full Table 5 is available in the HTML version of this article at http://www.g-cubed.org]

Sample	Depth, mm	[Nd], ppm	$^{143}Nd/^{144}Nd \pm 1\sigma$ SE	$\varepsilon_{Nd} \pm 2\sigma$ External Reproducibility	[Pb], ppm	$^{206}Pb/^{204}Pb$	$^{207}Pb/^{204}Pb$	$^{208}Pb/^{204}Pb$	$^{207}Pb/^{206}Pb$	$^{208}Pb/^{206}Pb$	[Sr], ppm
Crust 52CD-X											
1	0–1	330.2	0.512099 ± 3	−10.52 ± 0.51	1013	18.982	15.711	39.075	0.827649	2.058459	556
			0.512091 ± 2	−10.66 ± 0.51							
2	0–2	684.0	0.512097 ± 3	−10.56 ± 0.51	2445	18.968	15.708	39.064	0.827723	2.058491	1000
3	6–8	4.2	0.512567 ± 12	−1.38 ± 0.51	167	19.004	15.734	38.976	0.827499	2.050871	208
4	17–19	5.9	0.512817 ± 20	3.49 ± 0.80	39	18.905	15.668	38.778	0.828858	2.051277	375
5	23–24	2.5			10	18.897	15.713	38.938	0.831791	2.061064	417
6	35–36	6.1	0.512256 ± 8	−7.46 ± 0.51	41	18.988	15.711	39.051	0.827417	2.056548	520
7	44–47	4.0	0.512486 ± 10	−2.97 ± 0.51	13	19.038	15.756	39.140	0.827801	2.056263	423
8	61–67	7.0	0.512208 ± 7	−8.39 ± 0.51	21	19.004	15.712	39.078	0.826784	2.056329	196
			0.512183 ± 5	−8.88 ± 0.51							
9	69–70	13.7	0.512254 ± 7	−7.49 ± 0.51	29	18.981	15.713	39.052	0.827795	2.057331	316
Crust 52CD-a											
1		10.4	0.512143 ± 8	−9.66 ± 0.51	75	18.990	15.710	39.074	0.827319	2.057682	758
			0.512146 ± 5	−9.60 ± 0.51							
			0.512132 ± 4	−9.86 ± 0.51							
2		1.7	0.512302 ± 18	−6.56 ± 0.72	3	18.607	15.650	38.614	0.841111	2.075286	1460
3			0.512347 ± 27	−5.67 ± 1.08		18.832	15.677	38.820	0.832496	2.061505	990
4		4.0			2	18.402	15.649	38.428	0.850338	2.088168	1750
5			0.512490 ± 5	−2.89 ± 0.51	11	18.520	15.628	38.497	0.843851	2.078730	3100
			0.512364 ± 9	−5.34 ± 0.51							
Sample 95CD-1		28.3	0.512096 ± 4	−10.57 ± 0.51	51	19.150	15.732	39.161	0.821526	2.044937	482
			0.512141 ± 3	−9.69 ± 0.51							
Sample 18CD-0		20.6	0.512128 ± 7	−9.94 ± 0.51	52	19.003	15.708	39.064	0.826606	2.055658	710
			0.512169 ± 8	−9.15 ± 0.51							
Sample 83CD		8.6	0.512258 ± 7	−7.41 ± 0.51	8	19.076	15.729	39.132	0.824551	2.051266	1440
			0.512269 ± 5	−7.20 ± 0.51							
Sediment sample 52CD											
Oxalate leach			0.512341 ± 5	−5.80 ± 0.51		18.619	15.662	38.616	0.841197	2.073988	
6M HCl,			0.512650 ± 11	0.20 ± 0.51		18.760	15.670	38.770	0.835294	2.066611	
30min on hotplate											
HNO_3-HF			0.512650 ± 3	0.20 ± 0.51		18.882	15.666	38.847	0.829690	2.057342	
complete dissolution											
Sediment sample 51MC											
Oxalate leach			0.512875 ± 9	4.60 ± 0.51		18.594	15.649	38.479	0.841597	2.069413	
6M HCl,			0.512943 ± 4	5.90 ± 0.51		18.644	15.640	38.504	0.838896	2.065209	
30min on hotplate											
HNO_3-HF			0.512952 ± 4	6.10 ± 9.51		19.006	15.656	38.757	0.823745	2.039257	
complete dissolution											

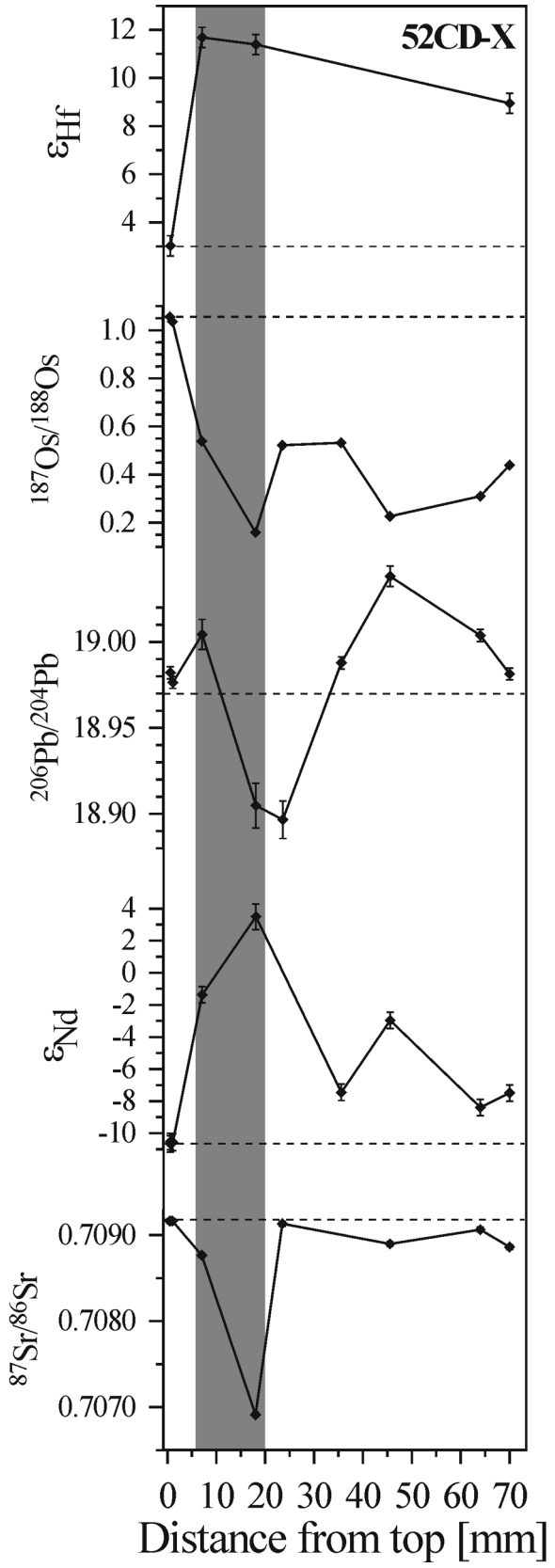

ferromanganese-coated sediments all show Sr isotope ratios close to seawater.

[20] Consistent with the Sr and Nd isotope results, $^{187}Os/^{188}Os$ shows the highest values of 1.05 in the hydrogenetic surface, essentially the same as present-day seawater [e.g., *Burton et al.*, 1999; *Peucker-Ehrenbrink and Ravizza*, 2000]. Significantly lower values are observed in the interior of this crust (Figure 6) and of 52CD-a. The minimum of 0.16, which is essentially the same as that of mantle rocks, again occurs in 52CD-X at a distance of 18 mm from the surface. The sediments with the ferromanganese matrix show $^{187}Os/^{188}Os$ indistinguishable from seawater.

[21] The Hf isotope composition was only measured on the outer hydrogenetic layer and on a few samples in the interior parts of crust 52CD-X that had high enough Hf concentrations. The ε_{Hf} value of the surface layer is +3. This is only slightly higher than in surfaces of hydrogenetic crusts from Blake Plateau in the Atlantic Ocean, presently bathed in Caribbean waters [*Godfrey et al.*, 1997; *David et al.*, 2001] and thus confirms a pure seawater origin also for Hf. ε_{Hf} reaches values of up to +11.7 in the interior of the crust, which is the highest so far observed Hf isotope value in ferromanganese crusts [*Godfrey et al.*, 1997; *van de Flierdt et al.*, 2004b], again similar to the signature of mantle rocks and the nearby island arc rocks. One value obtained for the ferromanganese matrix of the sediments shows a value significantly higher than that of seawater (ε_{Hf} = +6.7).

[22] By contrast, Pb isotopes in crust 52CD-X show a small variability. The isotope ratios in the hydrogenetic surface layer are not much different from the inner parts. This is remarkable in view of the fact that the Pb concentrations between the inner and hydrogenetic parts differ by a factor of up to 250 (Figure 7). In further contrast to the other isotope systems, the Pb isotope ratios of second crust 52CD-a vary significantly; e.g., $^{206}Pb/^{204}Pb$ ranges from 18.4 to 19.0 (Table 5). Thus the Pb

Figure 6. Sr, Nd, Pb, Os, and Hf isotope variations versus depth in crust 52CD-X. The dashed lines represent the inferred seawater isotope ratios for each isotope ratio. The gray bar marks the section with highest deviations from the seawater values. The error bars shown represent 2σ external reproducibilities. For some of the Pb isotope data only, where the internal error was larger than the external reproducibility due to low concentrations, the error bars stand for 2σ in run precision.

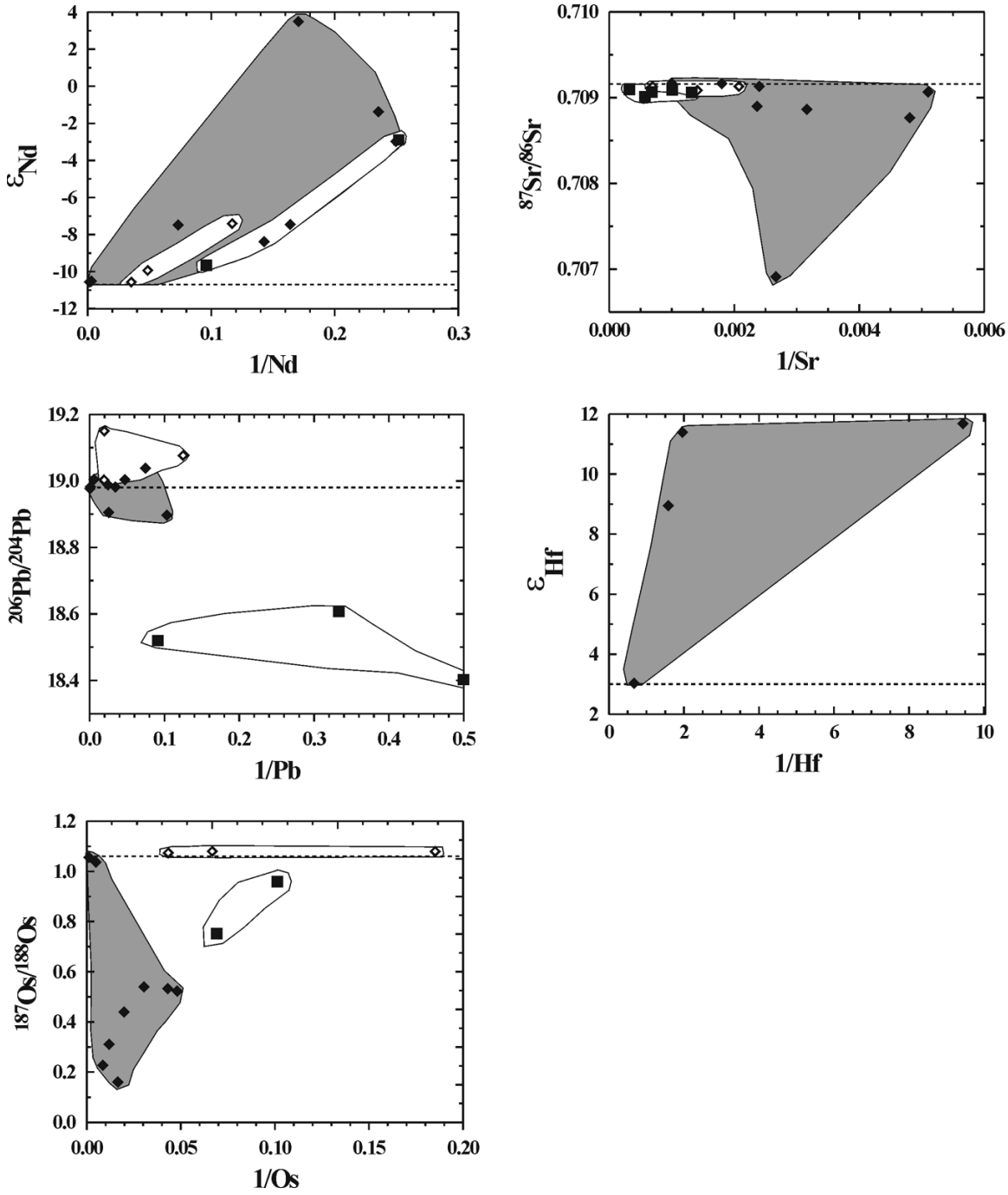

Figure 7. Correlations between the isotopic compositions and the concentrations of Nd, Sr, Pb, Os, and Hf in the crusts and the ferromanganese matrix of the sediment samples. The solid diamonds and the gray array mark the data of 52CD-X, the solid squares mark those of 52CD-a (white array), and the open diamonds mark those of the ferromanganese matrix of the sediment samples (18CD, 83CD, 95CD; white array). The dashed line marks the respective seawater isotope composition.

isotopes show patterns of variability which show no clear relationships with the other radiogenic isotope systems at all. The only exception may be that the lowest $^{206}Pb/^{204}Pb$ values correspond to the highest ε_{Nd} values in both massive crusts. The highest $^{206}Pb/^{204}Pb$ value is observed in the oxyhydroxide fraction of sediment sample 95CD-1 (19.14).

[23] Isotope ratios for all samples are plotted versus inverse concentrations to see if there are obvious

mixing relationships (Figure 7). Whereas for Sr, Os, and Hf concentrations are up to factors of 6, 28 and 25 higher, respectively, in the outer hydrogenetic layer than in the interior of crust 52CD-X, it is clear from these plots that only Nd shows a significant linear correlation and between concentration and isotopic composition for all data indicating mixing between two end-members, e.g., seawater and a hydrothermal component. For Os there is obviously a correlation for the interior parts of 52CD-X and 52CD-a, but the presumably most hydrothermally influenced parts show high concentrations, which probably indicates that the supply of Os with the hydrothermal fluids must have been very high resulting in a compensation of the dilution effect by the higher growth rates deduced for the other metals above. For Hf there may be a nonlinear relationship but we do not want to interpret this on the basis of only 4 data points. For Sr and Pb isotopes no obvious linear mixing relationships can be deduced from comparison of the available isotopic ratios and concentrations, indicating that additional factors other than simple mixing of the fluids with seawater controlled the element concentrations in the crusts.

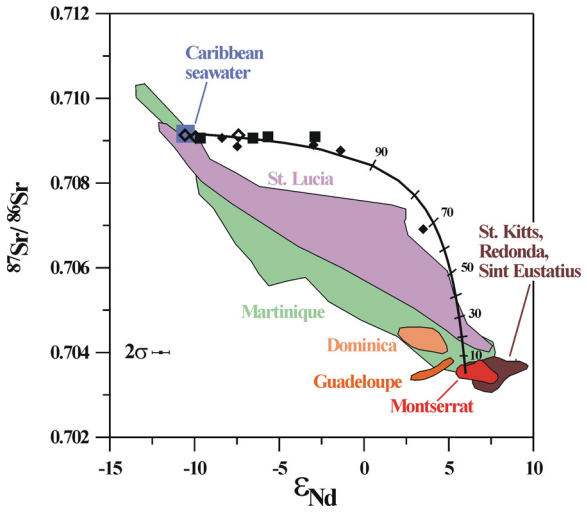

Figure 8. Comparison of the Nd and Sr isotope composition of the Caribbean crusts and the ferromanganese matrix of the sediment samples of this study with the composition of the nearby Lesser Antilles island arc rocks (sources can be found in the GEOROC database). The data are fitted by a mixing line between local seawater and an end-member composition close to that of rocks from Montserrat (solid line). The ticks and numbers indicate the amount of seawater contained in the mixture. Symbols are the same as in Figure 7. Error bars represent 2σ external reproducibilities.

4. Discussion

[24] To further evaluate mixing relationships between the fluids and seawater and to develop a genetic model for the occurrence of these crusts, the radiogenic isotope ratios in the crusts are compared with the respective isotopic compositions of those two end-members. For the seawater end-member, we will use the isotopic composition of the hydrogenetic surface layer of 52CD-X. For the hydrothermal end-member, we adopt the isotopic composition of the nearby islands of the Lesser Antilles island arc, essentially Montserrat, Guadeloupe and Dominica, as extracted from the GEOROC database (http://georoc.mpch-mainz.gwdg.de/georoc/), assuming that the hydrothermal fluids mainly derived their dissolved load from leaching of these island arc rocks and the island arc-derived sediments. This is probably an oversimplification because there may have been significant magmatic components from the mantle involved in the formation of the hydrothermal fluids, but for most of the radiogenic isotope systems considered in this study this approach can nevertheless be entertained because mantle and local arc rock-derived signatures are not largely different.

[25] Unambiguous quantitative estimates of contributions of Sr, Nd, Os and Hf from hydrothermal fluids versus seawater for the crusts and sediments of this study cannot be obtained. This is mainly because we do not know the partition coefficients between the fluids and the minerals of the crusts and also the end-member concentrations of these metals in the hydrothermal fluids that supplied the crusts, which have most likely been quite different from high-temperature hydrothermal fluids at MORs [*Gamo et al.*, 1997; *de Ronde et al.*, 2001, 2003], are not known. In order to nevertheless get an approximate idea of the order of magnitude of the hydrothermal contributions we did some calculations adopting a similar approach to that of *Mills and Elderfield* [1995].

4.1. Mixing Between Seawater and Fluids

4.1.1. Strontium

[26] For Sr we assumed the Sr isotope composition of the fluid end-member derived from leaching the nearby island arc rocks to have a Sr isotope ratio of 0.7035 (see Figure 8), which is essentially the same as a mantle signature. The end-member Sr concentration in seawater is 7.6 ppm, its Sr isotope ratio is known and for the hydrothermal fluids we chose an average value of 10.6 ppm [*Palmer and Edmond*,

1989]. Applying these values results in small hydrothermal fluid contributions to the Sr in the crusts between 0 and 2% in crust 52CD-a and in the sediments with the ferromanganese matrix and highest values on the order of 30% at 18 mm depth in crust 52CD-X, which suggests a close proximity of crust 52CD-X during growth of the hydrothermal layers to hydrothermal fluid sources. Again, these values are not considered reliable quantitative results because we assumed that the hydrothermal fluids that have supplied the hydrothermal crusts of this study had concentrations similar to mid ocean ridge high-temperature fluids, which was probably not the case. However, the data clearly suggest that parts of the interior of crust 52CD-X received significant amounts of Sr from hydrothermal solutions.

4.1.2. Neodymium

[27] The hydrothermal contributions to Nd, Os, and Hf are even more difficult to evaluate quantitatively. The range of concentrations of high-temperature hydrothermal fluids is very large or poorly known, which makes comparisons with the back arc hydrothermal fluids even more uncertain.

[28] For Nd, high-temperature hydrothermal fluids at mid-ocean ridges are enriched by factors between 10 and 400 compared with ambient seawater [*Mitra et al.*, 1994; *Klinkhammer et al.*, 1994] but Nd is rapidly scavenged near or within the vents [*German et al.*, 1990; *Halliday et al.*, 1992]. This implies that any hydrothermal Nd contributions in hydrothermal precipitates can only be found in immediate proximity to the vent sites. For a similar exercise as for Sr above, a seawater Nd concentration of 3.3 pg/g, a seawater ε_{Nd} of -10.7, and a hydrothermal end-member ε_{Nd} of 5.8 are realistic values. If Nd concentrations between 25 and 1200 pg/g [*Klinkhammer et al.*, 1994] as known for high-temperature MOR fluids are applied, a range of contributions from hydrothermal fluids between 45% and 2%, respectively, are calculated for the most hydrothermally influenced parts of crust 52CD-X. Even the lowest estimate of 2% indicates a large hydrothermal contribution compared to that found by *Mills et al.* [2001] for the only one hydrothermally influenced crust from the TAG hydrothermal field in the Atlantic Ocean that showed a significant deviation from the seawater signature in its Nd isotope composition. This confirmed a significant hydrothermal fraction of the Nd in this part of the crust, which was interpreted to have precipitated from low-temperature fluids.

[29] In Figure 8 the Sr and Nd isotope data of the crusts are plotted together with the isotopic composition of the island arc rocks and seawater. The northern islands of the arc, in particular Montserrat and Guadeloupe, which are closest to the location of the crusts are homogenous in their Sr and Nd isotope composition. All data plot near a binary mixing curve between the seawater end-member and the narrowly constrained fields of the northern islands. This indicates again that Sr and Nd in the Fe-Mn-oxyhydroxide phase of the samples of this study are mainly a two-component mixture between supplies from local seawater and hydrothermal fluids, which received their Nd and Sr from leaching of the island arc rocks.

[30] Whereas it is well known that Sr is supplied hydrothermally to the ocean, it has in the case of Nd so far only been observed once that the Nd isotope composition of hydrothermal ferromanganese crusts results from mixing of hydrothermal fluids and seawater [*Mills et al.*, 2001]. This one case was attributed to low-temperature fluids at the TAG hydrothermal field. In all other cases the Nd isotope composition of hydrothermal crusts have been shown to reflect essentially pure seawater [e.g., *Mills et al.*, 2001], even if Pb isotopes indicated significant hydrothermal contributions [*Vlastélic et al.*, 2001; *Albarède et al.*, 1997; *van de Flierdt et al.*, 2004b]. The above observations thus also lend support to the view that the temperatures of the fluids supplying the metals at the time of precipitation of the crusts of this study were probably relatively low.

Figure 9. Comparison of the Pb isotope composition of the Caribbean crusts and incrusted sediments with the composition of the Caribbean island arc rocks (sources of the data can be found in the GEOROC database) and other potential external sources in (top) $^{208}Pb/^{204}Pb$ versus $^{206}Pb/^{204}Pb$ and (bottom) $^{207}Pb/^{204}Pb$ versus $^{206}Pb/^{204}Pb$ space. The data for the Orinoco sediments are from *White et al.* [1985], those for Saharan dust as represented by the detrital fraction of eastern North Atlantic sediments are from *Sun* [1980], and the Saharan aerosol data are from B. Hamelin (personal communication, 2003). Local seawater composition is derived from the hydrogenetic surface layer of crust 52CD-X. Symbols are the same as in Figure 7. The crosses mark the results obtained from two different leaches and a complete dissolution of the residual material of the leaches (labeled "C") of sediment samples 52CD (gray symbols) from the same dredge as the two massive crusts and 51MC (black symbols) from a location nearby. Error bars are smaller than the size of the symbols.

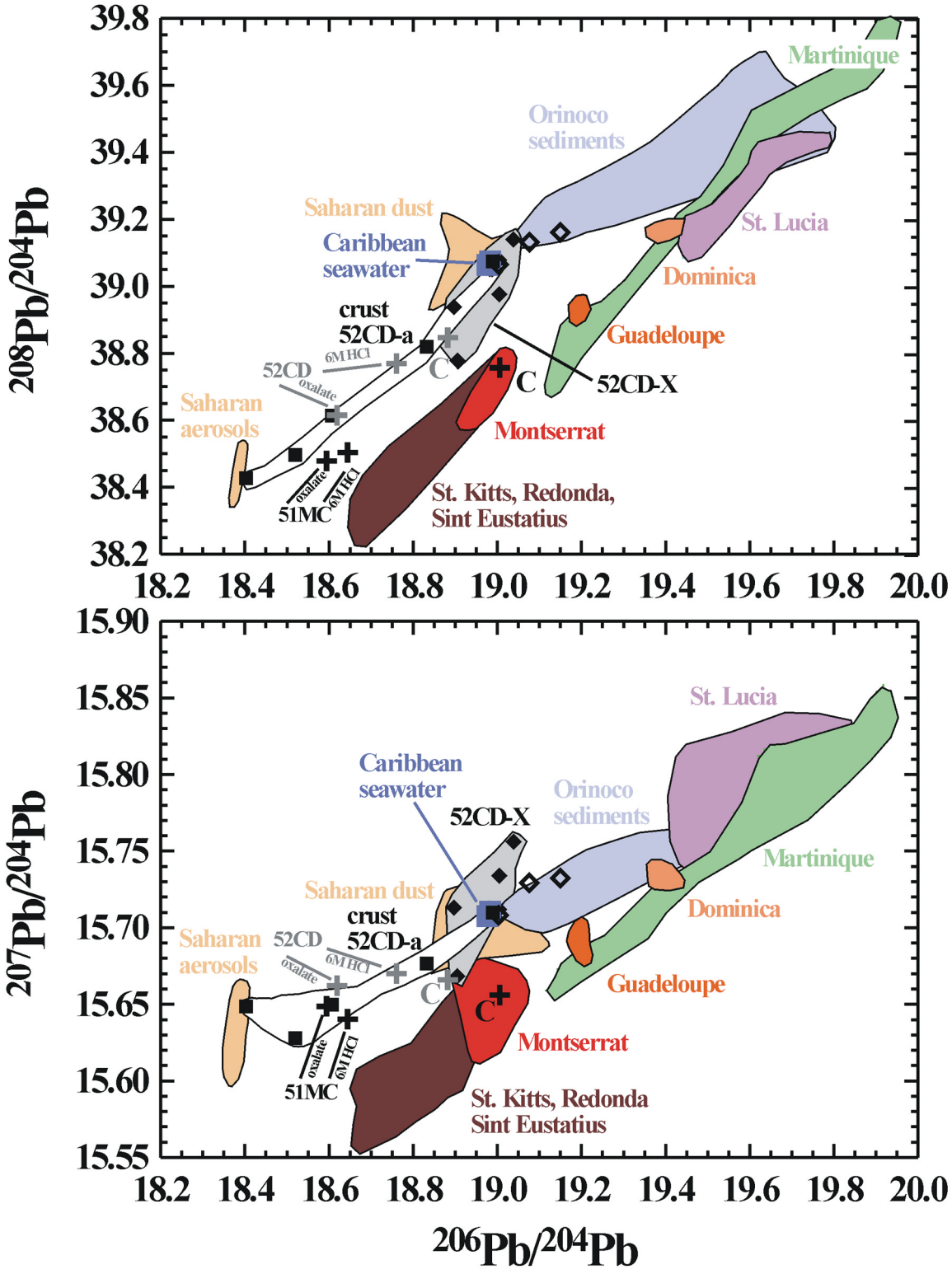
208Pb/204Pb
207Pb/204Pb
206Pb/204Pb
Martinique
Orinoco sediments
Saharan dust
Caribbean seawater
St. Lucia
Dominica
crust
52CD-a
6M HCl
52CD
oxalate
C
52CD-X
Guadeloupe
Saharan aerosols
Montserrat
St. Kitts, Redonda, Sint Eustatius
51MC

Figure 9

4.1.3. Osmium

[31] Hydrothermal contributions have been shown to play an important role for the seawater budget of Os [e.g., *Peucker-Ehrenbrink and Ravizza*, 2000]. Only few data are available for Os concentrations in hydrothermal vent fluids. They range between 2.8 and 38 pg/kg in high-temperature fluids, and up to 98 pg/kg in low-temperature fluids [*Sharma et al.*, 2000]. These concentrations are similar to the concentration of 11 pg/kg for seawater, which has a $^{187}Os/^{188}Os$ of 1.06 [*Levasseur et al.*, 1998]. The Os isotope composition of hydrothermal fluids at MORs was found to be similar to that of the basalts [*Sharma et al.*, 2000]. Other than for Sr and Nd a potential hydrothermal end-member isotope composition derived from leaching of the arc rocks is more difficult to estimate for Os because there are only very few data available. These few data show quite a significant scatter even for rocks within one island pointing to inhomogeneities caused by crustal contamination during ascent, or different amounts of sediments and altered oceanic crust incorporated into the melts during subduction-related melting [*Alves et al.*, 2002, *Woodland et al.*, 2002]. As the lowest $^{187}Os/^{188}Os$ value we measured in crust 52CD-X (0.16) is close to the low end for all measured values in these island arcs (and close to that found for the upper mantle of 0.12), we suggest that the hydrothermal fluids must have had a similar value, at least at this location. Applying hydrothermal end-member $^{187}Os/^{188}Os$ ratios between 0.12 and 0.15, and assuming a range in concentrations similar to results obtained previously [*Sharma et al.*, 2000], calculations of hydrothermal contributions yield a range from pure seawater composition to between 10 and 40% of the Os derived from the fluids in the most hydrothermally influenced parts.

4.1.4. Hafnium

[32] There are fewer constraints to estimate the hydrothermal Hf contributions to the crusts because the Hf concentrations and isotopic signatures in hydrothermal fluids are not known at all. A previous study based on Hf isotope measurements of ferromanganese crusts suggested that high-temperature hydrothermal fluids may supply amounts of Hf large enough to be important for the oceanic mass balance of Hf due to very radiogenic Hf isotope ratios found in two hydrothermal crusts [*Godfrey et al.*, 1997]. Results of a recent study suggested, however, that Hf is not supplied to seawater by high-temperature hydrothermal fluids in significant amounts. This was deduced from a missing reflection of Pb isotope-derived hydrothermal influence in the Hf isotope composition of the same mixed hydrothermal-hydrogenetic crust from the eastern equatorial Pacific Ocean [*van de Flierdt et al.*, 2004b].

[33] Comparison of the Hf isotope composition of the most hydrothermally influenced part of the crusts of this study (up to $\varepsilon_{Hf} = +11.7$) with the seawater value ($\varepsilon_{Hf} = +3$) and available data on the nearby island arc rock end-members, which mostly are in the ε_{Hf} range between +8 and +14 [*White and Patchett*, 1984; *Woodhead et al.*, 2001], confirms the results obtained from the other isotope systems: A significant proportion of the Hf in the most hydrothermally influenced sections must have originated from the hydrothermal fluids. Like the Nd and Sr isotopic compositions of the crusts (Figure 8), the data of this study also fall on a mixing line between seawater and Montserrat when Hf and Os isotope compositions are compared with those of Nd and Sr. However, the scatter around the mixing line in plots including Hf and Os isotopic compositions is greater than in Sr-Nd isotope space. This may either be caused by the less homogenous Os and Hf isotope compositions of the arc rocks or by factors other than two-component mixing between seawater and hydrothermal solutions, as already discussed in section 3.3 for the isotope/element relationships.

4.2. Lead

[34] Lead isotopes show markedly different results compared with the other four studied isotope systems. Hydrothermal inputs of Pb are known at MORs, from where they can be dispersed in deep waters over some distance and be incorporated into ferromanganese crusts [*Barrett et al.*, 1987; *Vlastélic et al.*, 2001; *van de Flierdt et al.*, 2004b]. End-member concentration measurements of Pb in high-temperature hydrothermal fluids range between 90 nmol/kg and 1650 nmol/kg [e.g., *von Damm et al.*, 1985; *Chen et al.*, 1986; *Hinkley and Tatsumoto*, 1987; *Godfrey et al.*, 1994; *Metz and Trefry*, 2000], compared with ambient deep-water concentrations of 0.05 nmol/kg. This results in Pb enrichment factors in hydrothermal fluids between 1,800 and 33,000.

[35] To estimate any hydrothermal Pb contributions to the crusts, we compare the Pb isotope composition of potential end-members with those of the hydrothermal crusts (Figure 9). The Pb isotope data of the rocks of the Lesser Antilles island arc plot along near linear arrays in

$^{208}Pb/^{204}Pb$ versus $^{206}Pb/^{204}Pb$ and $^{207}Pb/^{204}Pb$ versus $^{206}Pb/^{204}Pb$ space. In addition, there is a clear evolution of the particular islands from less radiogenic Pb isotope compositions in the north of the arc (St. Kitts, Redonda, Sint Eustatius) to more radiogenic compositions in the south, which has been interpreted as a consequence of the different amounts of subducted and recycled sediments that contributed to the formation of the arc rocks [*White and Dupré*, 1986; *MacDonald et al.*, 2000]. Essentially all the Pb isotope data obtained from the studied crusts define a near linear array parallel to the array for the island arc rocks in Figure 9. They do also not fall between the seawater end-member and the Pb isotope composition of any of the islands, which excludes mixing of Pb from local seawater with Pb originating from weathering of the island arcs as explanation for the observed isotope patterns (Figure 9).

[36] Comparison of the Caribbean seawater Pb isotope composition with Atlantic seawater signatures, as derived from surfaces and time series of hydrogenetic crusts from the western Atlantic Ocean [*von Blanckenburg et al.*, 1996b; *Burton et al.*, 1997; *Reynolds et al.*, 1999], essentially excludes Atlantic seawater as the main factor controlling the Pb isotope composition of Caribbean seawater. All Atlantic seawater Pb isotope data (not included in Figure 8) fall on the same arrays as the island arc rocks and are clearly different from local seawater. This makes sense in view of the short residence time of Pb in seawater that prevents long-distance advection of isotopic signals. It is noteworthy in that respect that the Pb isotope composition of Caribbean seawater is very similar to the data for Saharan dust, which may indicate that dissolution of dust has been an important contributor.

[37] Thus at least two additional external end-members must have been involved, which is reflected by the well-defined linear array of the data of crust 52CD-a. To the radiogenic end, Pb originating from the Orinoco River particulates would be suitable, as evidenced by the radiogenic Pb isotope composition of the detrital fraction of sediments from the Barbados Ridge-Demerara Plain region [*White et al.*, 1985] (Figure 9). This is supported by the fact that river waters and suspended detrital particles supplied by the Orinoco River flow north along the South American coast and into the Caribbean [e.g., *Müller-Karger et al.*, 1989; *Nesbitt and Young*, 1997]. An alternative radiogenic Pb contributor is Saharan dust which is known to be supplied to the Caribbean in large quantities [*Hamelin et al.*, 1989] and which also has a suitable natural Pb isotope composition as indicated by data obtained from the detrital fraction of eastern North Atlantic sediments [*Sun*, 1980] (Figure 9). The mixing end-member with low (unradiogenic) Pb isotope ratios is more difficult to constrain but it is well possible that the few bulk detrital sediment data provided by *Sun* [1980] do not cover the entire range of the Pb isotope composition of Saharan dust given that Saharan rocks are very heterogeneous with respect to their age and genesis. In Figure 9 the Pb isotope compositions of two aerosol samples (B. Hamelin and A. Véron, personal communication, 2005) with a very unradiogenic Pb isotope composition originating from the Western Sahara are plotted together with the other Pb isotope data. In contrast to anthropogenically contaminated aerosol samples analyzed in many previous studies [e.g., *Hamelin et al.*, 1989], these new data are interpreted to reflect the natural Pb isotope composition of Saharan aerosols because their Pb/Al ratios do not show an anthropogenic enrichment and because their Pb isotope compositions are consistent with that of the residual fraction of marine particles collected near the Cape Verde islands and in the Ligurian Sea [*Journel et al.*, 1998]. These uncontaminated aerosol signatures plot exactly where the unradiogenic mixing end-member composition for the data of crust 52CD-a is expected.

[38] Only very small amounts of Pb are found in the hydrothermally influenced ferromanganese matrix of the interior layers. Thus, if only a small amount of the labile aerosol dust-derived Pb was leached during the applied chemical procedures, then this would dominate the Pb isotopes and explain the observed patterns in Figure 9. This hypothesis is further confirmed by Pb isotope analyses performed on leachates of one sediment sample recovered from the same dredge as the crusts (52CD) and one sediment sample from a distance of only a few km away (51MC). These sediment samples, the detrital fraction of which probably consists to some extent of Saharan dust, were subjected to a weak leach in an oxalate cocktail at room temperature [*Tovar-Sanchez et al.*, 2003] and a stronger leach for 30 min in hot 6 M HCl, similar to the method used to dissolve the crusts and the residue was finally completely dissolved. All radiogenic isotope data for the completely dissolved residue are consistent with an island arc rock origin. The Pb isotope data of the two different leaches, however, plot on or near the

array defined by the data of crust 52CD-a (Figure 9), thus supporting the above suggestion that the Pb in the interior part of CD52-a is dominated by Pb leached from Saharan dust.

[39] Alternatively, it may also be possible that Pb in the detrital, island arc rock-derived particles of the two sediment samples as well as in the crusts are not released with the same Pb isotope composition as the bulk composition during the leaching procedures. Such an incongruent release of Pb isotopes has been demonstrated for examples for old continental rocks in the North Atlantic region [*von Blanckenburg and Nägler*, 2001] and for Asian loess [*Jones et al.*, 2000; *Ling et al.*, 2005]. This is consistent with the trend from the Pb isotope composition of the completely dissolved residue, via the strong 6 M HCl leach to the weakest leach which may indicate preferential dissolution of some labile unradiogenic phase. This must, however, remain speculative because no other data exist on leaching experiments for Pb isotopes in Saharan dust or island arc volcanics.

[40] In summary, the Pb measured in the 6M HCl leach of the hydrothermally influenced crusts cannot be derived from hydrothermal fluids but most likely originates from leaching of the detrital particles incorporated in the crusts.

4.3. Constraints on the Origin and Temperature of the Hydrothermal Fluids

[41] Our preferred mechanism to explain the observed radiogenic isotope patterns is a reaction between the ascending hydrothermal fluids and the sediments overlying the vent sites. Such interactions have been described by observational as well as experimental studies. In the case of Pb, observations similar to the ones made in our study have been made in the Escabana Trough in the northeast Pacific. There it was shown that the Pb isotopes of the vent fluids are dominated by the signature of the overlying sediments while the original Pb isotope signature emanating from the underlying basalts was probably removed at the sediment/basalt interface by sulfide precipitation [*LeHuray et al.*, 1988; *German et al.*, 1995]. In contrast to the Escabana Trough situation where Nd and Sr in the hydrothermal sediments were dominated by seawater, the results of our study show that Nd and Sr, as well as Os and Hf in the hydrothermal parts of the crusts were significantly influenced by either metal contributions from the mantle or, more likely, by metals derived from leaching of the island arc rocks. The metals with the island arc isotope signature either had their source in the original hydrothermal vent fluids or, alternatively, in the hydrothermal leaching of the island-arc-derived detrital sediment cover by the fluids. The temperature of the fluids probably played a major role in creating the isotopic signature of the oxyhydroxide precipitates. Experiments have for example shown that the amount of Pb leached from sediments by hydrothermal fluids is very low at temperatures of 275°C and below [*Cruse and Seewald*, 2003]. This implies that significant amounts of Nd, Sr, Os and Hf were leached from the arc-derived sediments, whereas the temperatures were not high enough for Pb, the isotope composition of which is consequently dominated by other sources (leaching of dust). In support of this hypothesis, it has recently been shown by laboratory experiments that Sr can indeed be leached from oceanic crust and overlying sediments by low-temperature hydrothermal fluids [*James et al.*, 2003].

[42] The results of this study show a clear hydrothermal influence on the crusts of this study, including a strong signal in the isotope composition of Nd, which is generally seawater-dominated in hydrothermal crusts. This may indicate that low-temperature hydrothermal fluid inputs in back arc basins and probably also low-temperature hydrothermal systems at MORs [e.g., *Mills et al.*, 2001] can be an important source of trace metals in seawater, even for metals such as Nd, which are not supplied to the ocean by high-temperature MOR hydrothermal systems. This remains to be verified, however, by analyses of the content and isotopic composition of such metals in the fluids themselves.

5. Conclusions

[43] Combined evidence from radiogenic isotope compositions, major and minor element content, as well as mineralogical data demonstrates varying hydrothermal contributions to massive, sediment-hosted, submarine ferromanganese crusts recovered near the Lesser Antilles island arc. The hydrothermal fluids responsible for the formation of the crusts most likely had relatively low temperatures by the time of precipitation as evidenced from rhythmically precipitated todorokite minerals with bladed structures, as well as REE patterns and the radiogenic isotope distributions. A thin layer of hydrogenetic crust covering the hydrothermal section of the crusts suggests that hydrothermal activity at the location on Montserrat Ridge stopped

several 100 kyr ago, as deduced from ^{10}Be concentrations. Supported by estimates of growth rates in the inner parts of the crusts, as obtained by Co-constant-flux modeling, it is suggested that the period of hydrothermal activity and growth of the hydrothermal part of the crust occurred within a relatively short period of activity of only a few tens of kyr.

[44] The relative amounts of metals in the crusts originating from seawater and hydrothermal fluids were estimated based on known metal concentrations of high-temperature hydrothermal fluids and the radiogenic isotope compositions of the crusts. These estimates can only be considered very rough because back-arc hydrothermal fluids may have very different and unknown compositions of the metals of this study [*Gamo et al.*, 1997; *de Ronde et al.*, 2001, 2003]. Nevertheless it is clear that significant hydrothermal contributions of Sr, Nd, Os and Hf to the crusts occurred, most likely originating from leaching of the arc-derived sediments overlying the hydrothermal sites.

[45] The Pb isotope data cannot be explained by mixing between seawater and island arc rock signatures. The absence of a hydrothermal Pb isotope signal is most likely related to the relatively low temperatures of the fluids from which the crusts precipitated. External sources, most likely leaching of particulates originating from the Orinoco River and Saharan dust, possibly even incongruent release of Pb isotopes from the island arc rock-derived sediments, have dominated the small amounts of Pb that were leached with 6 M HCl from the hydrothermal sections of the crusts.

[46] With the exception of Pb, the radiogenic isotope data may indicate that hydrothermal inputs via hydrothermal fluids related to island arc volcanism might be an important source of metals in seawater, which need to be verified by detailed future geochemical and isotopic studies of such fluids.

Acknowledgments

[47] Research cruise SO 154 was funded by the German Bundesministerium für Bildung und Forschung (project 03 G 0154 A). We would like to thank C. German and D. Teagle for discussions and B. Peucker-Ehrenbrink and C.E.J. de Ronde for comments on a previous version of this manuscript. R. Mills, J.D. Gleason, and an anonymous reviewer are thanked for their thoughtful reviews. The Southampton Oceanography centre is thanked for the measurements of REE and minor element concentrations. C. Stirling, H. Williams, S. Woodland, M. Rehkämper, F. Oberli, H. Baur, M. Maier, U. Menet, D. Niederer, B. Rütsche, and A. Süsli are thanked for their help in keeping the mass spectrometers running smoothly as well as for clean lab and computer support.

References

Albarède, F., S. L. Goldstein, and D. Dautel (1997), The neodymium isotopic composition of manganese nodules from the Southern and Indian oceans, the global oceanic neodymium budget, and their bearing on deep ocean circulation, *Geochim. Cosmochim. Acta*, *61*, 1277–1291.

Alves, S., P. Schiano, F. Capmas, and C. J. Allègre (2002), Osmium isotope binary mixing arrays in arc volcanism, *Earth Planet. Sci. Lett.*, *198*, 355–369.

Axelsson, M. D., I. Rodushkin, J. Ingri, and B. Öhlander (2002), Multielemental analysis of Mn-Fe nodules by ICP-MS: Optimisation of analytical method, *Analyst*, *127*, 76–82.

Baker, E. T., G. J. Massoth, K. Nakamura, R. W. Embley, C. E. J. de Ronde, and R. J. Arculus (2005), Hydrothermal activity on near-arc sections of back-arc ridges: Results from the Mariana Trough and Lau Basin, *Geochem. Geophys. Geosyst.*, *6*, Q09001, doi:10.1029/2005GC000948.

Barrett, T. J., P. N. Taylor, and J. Lugowski (1987), Metalliferous sediments from DSDP Leg 92: The East Pacific Rise transect, *Geochim. Cosmochim. Acta*, *51*, 2241–2253.

Belshaw, N. S., P. A. Freedman, R. K. O'Nions, M. Frank, and Y. Guo (1998), A new variable dispersion double-focussing plasma mass spectrometer with performance illustrated for Pb-isotopes, *Int. J. Mass Spectrom.*, *181*, 51–58.

Birck, J. L., M. Roy-Barman, and F. Capmas (1997), Re-Os isotopic measurements at the femtomole level in natural samples, *Geostand. Newsl.*, *21*, 19–27.

Bourlès, D. L., G. M. Raisbeck, E. T. Brown, F. Yiou, and J. M. Edmond (1991), Beryllium isotope systematics of submarine hydrothermal systems, *Earth Planet. Sci. Lett.*, *105*, 534–542.

Bourlès, D. L., E. T. Brown, C. R. German, C. I. Measures, J. M. Edmond, G. M. Raisbeck, and F. Yiou (1994), Examination of hydrothermal influences on oceanic beryllium using fluids, plume particles and sediments from the TAG hydrothermal field, *Earth Planet. Sci. Lett.*, *122*, 143–157.

Burton, K. W., H.-F. Ling, and R. K. O'Nions (1997), Closure of the Central American Isthmus and its effect on deep-water formation in the North-Atlantic, *Nature*, *386*, 382–385.

Burton, K. W., B. Bourdon, J.-L. Birck, C. J. Allègre, and J. R. Hein (1999), Osmium isotope variations in the oceans recorded by Fe-Mn crusts, *Earth Planet Sci. Lett.*, *171*, 185–197.

Chen, J. H., G. J. Wasserburg, K. L. von Damm, and J. M. Edmond (1986), The U-Th-Pb systematics in hot springs on the East Pacific Rise at 21°N and Guyamas Basin, *Geochim. Cosmochim. Acta*, *50*, 2467–2479.

Cohen, A. S., R. K. O'Nions, R. Siegenthaler, and W. L. Griffin (1988), Chronology of the pressure-temperature history recorded by a granulite terrain, *Contrib. Mineral. Petrol.*, *98*, 303–311.

Creaser, R. A., D. A. Papanastassiou, and G. J. Wasserburg (1991), Negative thermal ion mass-spectrometry of osmium, rhenium, and iridium, *Geochim. Cosmochim. Acta*, *55*, 397–401.

Cruse, A. M., and J. S. Seewald (2003), Metal mobility in sediment covered ridge-crest hydrothermal systems: Experimental and theoretical constraints, *Geochim. Cosmochim. Acta*, *65*, 3233–3247.

David, K., M. Frank, R. K. O'Nions, N. S. Belshaw, J. W. Arden, and J. R. Hein (2001), The Hf isotope composition of global seawater and the evolution of Hf isotopes in the deep Pacific Ocean from Fe-Mn crusts, *Chem. Geol.*, *178*, 23–42.

de Ronde, C. E. J., E. T. Baker, G. J. Massoth, J. E. Lupton, I. C. Wright, R. A. Feely, and R. R. Greene (2001), Intra-oceanic subduction-related hydrothermal venting, Kermadec volcanic arc, New Zealand, *Earth Planet. Sci. Lett.*, *193*, 359–369.

de Ronde, C. E. J., K. Faure, C. J. Bray, D. Chappell, and I. C. Wright (2003), Hydrothermal fluids associated with seafloor mineralization at two southern Kermadec arc volcanoes, offshore New Zealand, *Miner. Deposita*, *38*, 217–233.

Devine, J. D., and H. Sigurdsson (1995), Petrology and eruption styles of Kick'em-Jenny submarine volcano, Lesser Antilles island arc, *J. Volcanol. Geotherm. Res.*, *69*, 35–58.

Douville, E., P. Bienvenu, J. L. Charlou, J. P. Donval, Y. Fouquet, P. Appriou, and T. Gamo (1999), Yttrium and rare earth elements in fluids from various deep-sea hydrothermal systems, *Geochim. Cosmochim. Acta*, *63*, 627–643.

Elderfield, H., C. J. Hawkesworth, M. J. Greaves, and S. E. Calvert (1981), Rare earth element geochemistry of oceanic ferromanganese nodules and associated sediments, *Geochim. Cosmochim. Acta*, *45*, 513–528.

Fink, L. K. (1972), Bathymetric and geologic studies of the Guadeloupe region, Lesser Antilles island arc, *Mar. Geol.*, *12*, 267–288.

Frank, M. (2002), Radiogenic isotopes: Tracers of past ocean circulation and erosional input, *Rev. Geophys.*, *40*(1), 1001, doi:10.1029/2000RG000094.

Frank, M., R. K. O'Nions, J. R. Hein, and V. K. Banakar (1999), 60 Ma records of major elements and Pb-Nd isotopes from hydrogenous ferromanganese crusts: Reconstruction of seawater paleochemistry, *Geochim. Cosmochim. Acta*, *63*, 1689–1708.

Frank, M., T. van de Flierdt, A. N. Halliday, P. W. Kubik, B. Hattendorf, and D. Günther (2003), The evolution of deep water mixing and weathering inputs in the central Atlantic Ocean over the past 33 Myr, *Paleoceanography*, *18*(4), 1091, doi:10.1029/2003PA000919.

Galer, S. J. G., and W. Abouchami (1998), Practical application of lead triple spiking for correction of instrumental mass discrimination, *Min. Mag.*, *62A*, 491–492.

Gamo, T., K. Okamura, J.-L. Charlou, T. Urabe, J.-M. Auzende, J. Ishibashi, K. Shitashima, H. Chiba, and Manus-Flux Cruise Shipboard Scientific Party (1997), Acidic and sulphate-rich hydrothermal fluids from the Manus back-arc basin, Papua New Guinea, *Geology*, *25*, 139–142.

German, C. R., G. P. Klinkhammer, J. M. Edmond, A. Mitra, and H. Elderfield (1990), Hydrothermal scavenging of rare-earth elements in the ocean, *Nature*, *345*, 516–518.

German, C. R., B. A. Barreiro, N. C. Higgs, T. A. Nelsen, E. M. Ludford, and M. R. Palmer (1995), Seawater-metasomatism in hydrothermal sediments (Escabana Trough, northeast Pacific), *Chem. Geol.*, *119*, 175–190.

Godfrey, L. V., R. Mills, H. Elderfield, and E. Gurvich (1994), Lead behaviour at the TAG hydrothermal vent field, 26°N, Mid-Atlantic Ridge, *Mar. Chem.*, *46*, 237–254.

Godfrey, L. V., D.-C. Lee, W. F. Sangrey, A. N. Halliday, V. J. M. Salters, J. R. Hein, and W. M. White (1997), The Hf isotopic composition of ferromanganese nodules and crusts and hydrothermal manganese deposits: Implications for seawater Hf, *Earth Planet. Sci. Lett.*, *151*, 91–105.

Günther, D., I. Horn, and B. Hattendorf (2000), Recent trends and developments in laser ablation-ICP-mass spectrometry, *Fresenius J. Anal. Chem.*, *368*, 4–14.

Halbach, P., H. Marbler, D. S. Cronan, A. Koschinsky, E. Rahders, and R. Seifert (2002), Submarine hydrothermal mineralisations and fluids off the Lesser Antilles island arc—Initial results from the CARIBFLUX cruise SO 154, *InterRidge News*, *11*, 18–22.

Halliday, A. N., J. P. Davidson, P. Holden, R. M. Owen, and A. M. Olivarez (1992), Metalliferous sediments and the scavenging residence time of Nd near hydrothermal vents, *Geophys. Res. Lett.*, *19*, 761–764.

Hamelin, B., F. E. Grousset, P. E. Biscaye, and A. Zindler (1989), Lead isotopes in trade wind aerosols at Barbados: The influence of European emissions over the North Atlantic, *J. Geophys. Res.*, *94*, 16,243–16,250.

Hein, J. R., A. Koschinsky, P. Halbach, F. T. Manheim, M. Bau, J. K. Kang, and N. Lubick (1997), Iron and manganese oxide mineralisation in the Pacific, *Geol. Soc. Spec. Publ.*, *119*, 123–138.

Henken-Mellies, W. U., J. Beer, F. Heller, K. J. Hsü, C. Shen, G. Bonani, H. J. Hofmann, M. Suter, and W. Wölfli (1990), ^{10}Be and ^{9}Be in South Atlantic DSDP site 519: Relation to geomagnetic reversals and to sediment composition, *Earth Planet. Sci. Lett.*, *98*, 267–276.

Hinkley, T. K., and M. Tatsumoto (1987), Metals and isotopes in Juan de Fuca Ridge hydrothermal fluids and their associated solid materials, *J. Geophys. Res.*, *92*, 11,400–11,410.

Hodkinson, R. A., P. Stoffers, J. Scholten, D. S. Cronan, G. Jeschke, and T. D. S. Rogers (1994), Geochemistry of hydrothermal manganese deposits from the Pitcarin Island hotspot, southeastern Pacific, *Geochim. Cosmochim. Acta*, *58*, 5011–5029.

Horwitz, E. P., R. Chiarizia, and M. L. Dietz (1992), A novel strontium-selective extraction chromatographic resin, *Solvent Extr. Ion Exch.*, *10*, 313–336.

James, R. H., D. E. Allen, and D. E. Seyfried (2003), An experimental study of alteration of oceanic crust and terrigenous sediment at moderate temperatures (51 to 350°C): Insights as to chemical processes in near-shore ridge flank hydrothermal systems, *Geochim. Cosmochim. Acta*, *67*, 681–691.

Johnson, A., and D. S. Cronan (2001), Hydrothermal metalliferous sediments and waters off the Lesser Antilles, *Mar. Georesour. Geotechnol.*, *19*, 65–83.

Jones, C. E., A. N. Halliday, D. K. Rea, and R. M. Owen (2000), Eolian inputs of lead into the North Pacific, *Geochim. Cosmochim. Acta*, *64*, 1405–1416.

Journel, B., L. Y. Alleman, E. Nicolas, A. Véron, and B. Hamelin (1998), Stable lead isotopes contribution to the chemical climatology of the western Mediterranean, *Ann. Geophys.*, *16*, 729.

Klemm, V., S. Levasseur, M. Frank, J. R. Hein, and A. N. Halliday (2005), Osmium isotope stratigraphy of a marine ferromanganese crust, *Earth Planet. Sci. Lett.*, *238*, 42–48.

Klinkhammer, G. P., H. Elderfield, J. M. Edmond, and A. Mitra (1994), Geochemical implications of rare earth element patterns in hydrothermal fluids from mid-ocean ridges, *Geochim. Cosmochim. Acta*, *58*, 5105–5113.

Koschinsky, A., A. Stascheit, M. Bau, and P. Halbach (1997), Effects of phosphatization on the geochemical and mineralogical composition of marine ferromanganese crusts, *Geochim. Cosmochim. Acta*, *61*, 4079–4094.

Koschinsky, A., P. Halbach, S. Sander, W. Michaelis, and R. Seifert (2002), Hydrothermal fluids in the North Fiji Basin and Lesser Antilles, *Geochim. Cosmochim. Acta*, *66*(15A), A412.

Ku, T. L., M. Kusakabe, C. I. Measures, J. R. Southon, G. Cusimano, J. S. Vogel, D. E. Nelson, and S. Nakaya

(1990), Beryllium isotope distribution in the western North Atlantic: A comparison to the Pacific, *Deep Sea Res., Part A*, *37*, 795–808.

Kuhn, T., M. Bau, N. Blum, and P. Halbach (1998), Origin of negative Ce anomalies in mixed hydrothermal-hydrogenetic Fe-Mn crusts from the Central Indian Ridge, *Earth Planet. Sci. Lett.*, *163*, 207–220.

Lee, D.-C., A. N. Halliday, J. R. Hein, K. W. Burton, J. N. Christensen, and D. Günther (1999), Hafnium isotope stratigraphy of ferromanganese crusts, *Science.*, *285*, 1052–1054.

LeHuray, A. P., S. E. Church, R. A. Koski, and R. M. Bouse (1988), Pb isotopes in sulfides from mid-ocean ridge hydrothermal sites, *Geology*, *16*, 362–365.

Levasseur, S., J.-L. Birck, and C. J. Allègre (1998), Direct measurement of femtomoles of osmium and $^{187}Os/^{186}Os$ ratio in seawater, *Science*, *282*, 272–274.

Ling, H.-F., S.-Y. Jiang, M. Frank, H.-Y. Zhou, F. Zhou, Z.-L. Lu, X.-M. Chen, Y.-H. Jiang, and C. D. Ge (2005), Differing controls over the Cenozoic Pb and Nd isotope evolution of deepwater in the central North Pacific Ocean, *Earth Planet. Sci. Lett.*, *232*, 345–361.

Lowell, R. P., P. A. Rona, and R. P. von Herzen (1995), Seafloor hydrothermal systems*J. Geophys. Res.*, *100*, 327–352.

Lugmaier, G. W., and S. J. G. Galer (1992), Age and isotopic relationships among the angrites Lewis cliff 86010 and Angra dos Reis, *Geochim. Cosmochim. Acta*, *56*, 1673–1694.

MacDonald, R., C. J. Hawkesworth, and E. Heath (2000), The Lesser Antilles volcanic chain: A study in arc magmatism, *Earth Sci. Rev.*, *49*, 1–76.

Manheim, F. T. (1986), Marine cobalt resources, *Science*, *232*, 600–608.

Maury, R. C., K. Westbrook-Graham, P. E. Baker, P. Bouysse, and D. Westercamp (1990), Geology of the Lesser Antilles, in *The Geology of North America*, vol. H, *The Caribbean Region*, edited by G. Dengo and J. E. Case, pp. 141–166, Geol. Soc. of Am., Boulder, Colo.

McLennan, S. M. (1989), Rare earth elements in sedimentary rocks: Influence of provenance and sedimentary processes, in *Geochemistry and Mineralogy of Rare Earth Elements*, edited by B. R. Lipin and G. A. McKay, *Rev. Mineral.*, *21*, 169–200.

Metz, S., and J. H. Trefry (2000), Chemical and mineralogical influences on concentrations of trace metals in hydrothermal fluids, *Geochim. Cosmochim. Acta*, *64*, 2267–2279.

Mills, R. A., and H. Elderfield (1995), Rare earth element geochemistry of hydrothermal deposits from the active TAG Mound, 26°N Mid-Atlantic Ridge, *Geochim. Cosmochim. Acta*, *59*, 3511–3524.

Mills, R. A., D. M. Wells, and S. Roberts (2001), Genesis of ferromanganese crusts from the TAG hydrothermal field, *Chem. Geol.*, *176*, 283–293.

Mitra, A., H. Elderfield, and M. J. Greaves (1994), Rare earth elements in submarine hydrothermal fluids and plumes from the Mid-Atlantic Ridge, *Mar. Chem.*, *46*, 217–235.

Müller-Karger, F. E., C. R. McClain, T. R. Fisher, W. E. Esaias, and R. Varela (1989), Pigment distribution in the Caribbean Sea: Observations from space, *Prog. Oceanogr.*, *23*, 23–64.

Nesbitt, H. W., and G. M. Young (1997), Sedimentation in the Venezuela Basin, circulation in the Caribbean Sea, and the onset of Northern Hemisphere glaciation, *J. Geol.*, *105*, 531–544.

Palmer, M. R., and J. M. Edmond (1989), The strontium isotope budget of the modern ocean, *Earth Planet. Sci. Lett.*, *92*, 11–26.

Percival, J. B., and D. E. Ames (1993), Clay mineralogy of active hydrothermal chimneys and an associated mound, middle valley, northern Juan-de-Fuca Ridge, *Can. Mineral.*, *31*, 957–971.

Peucker-Ehrenbrink, B., and G. Ravizza (2000), The marine osmium isotope record, *Terra Nova*, *12*, 205–219.

Polyak, B. G., et al. (1992), Evidence of submarine hydrothermal discharge to the northwest of Guadeloupe Island (Lesser Antilles island arc), *J. Volcanol. Geotherm. Res.*, *54*, 81–105.

Reynolds, B. C., M. Frank, and R. K. O'Nions (1999), Nd- and Pb- isotope time series from Atlantic ferromanganese crusts: Implications for changes in provenance and paleocirculation over the last 8 Myr, *Earth Planet. Sci. Lett.*, *173*, 381–396.

Rimskaya-Korsakova, M. N., and A. V. Dubinin (2003), Rare earth elements in sulfides of submarine hydrothermal vents of the Atlantic Ocean, *Dokl. Earth Sci.*, *389A*, 432–436.

Sander, S., A. Koschinsky, and P. Halbach (2003), Redox-speciation of chromium in the oceanic water column of the Lesser Antilles and offshore Otago Peninsula, New Zealand, *Mar. Freshwater Res.*, *54*, 745–754.

Seyfried, W. E., Jr., J. S. Seewald, M. E. Berndt, K. Ding, and D. I. Foustoukos (2003), Chemistry of hydrothermal vent fluids from the Main Endeavour Field, northern Juan de Fuca Ridge: Geochemical controls in the aftermath of June 1999 seismic events, *J. Geophys. Res.*, *108*(B9), 2429, doi:10.1029/2002JB001957.

Sharma, M., G. J. Wasserburg, A. W. Hofmann, and D. A. Butterfield (2000), Osmium isotopes in hydrothermal fluids from the Juan de Fuca Ridge, *Earth Planet. Sci. Lett.*, *179*, 139–152.

Sun, S. S. (1980), Lead isotopic study of young volcanic rocks from mid-ocean ridges, ocean islands and island arcs, *Philos. Trans. R. Soc. London, Ser. A*, *297*, 409–445.

Tovar-Sanchez, A., S. A. Sanudo-Wilhelmy, M. Garcia-Vargas, R. S. Weaver, L. C. Popels, and D. A. Hutchins (2003), A trace metal clean reagent to remove surface-bound iron from marine phytoplankton, *Mar. Chem.*, *82*, 91–99.

Usui, A., and A. Nishimura (1992), Hydrothermal manganese oxide deposits from the Izu-Ogasawara (Bonin)-Mariana Arc and adjacent areas, *Bull. Geol. Surv. Jpn.*, *43*, 257–284.

Usui, A., T. A. Mellin, M. Nohara, and M. Yuasa (1988), Structural stability of marine 10Å manganates from the Ogasawara (Bonin) Arc: Implication for low temperature hydrothermal activity, *Mar. Geol.*, *86*, 41–56.

van de Flierdt, T., M. Frank, A. N. Halliday, J. R. Hein, B. Hattendorf, D. Günther, and P. W. Kubik (2003), Lead isotopes in North Pacific Deep Water: Implications for past changes in input sources and circulation patterns, *Earth Planet. Sci. Lett.*, *209*, 149–164.

van de Flierdt, T., M. Frank, A. N. Halliday, J. R. Hein, B. Hattendorf, D. Günther, and P. W. Kubik (2004a), Deep and bottom water export from the Southern Ocean to the Pacific Ocean over the past 38 million years, *Paleoceanography*, *19*, PA1020, doi:10.1029/2003PA000923.

van de Flierdt, T., M. Frank, A. N. Halliday, J. R. Hein, B. Hattendorf, D. Günther, and P. W. Kubik (2004b), Tracing the history of submarine hydrothermal inputs and the significance of hydrothermal hafnium for the seawater budget: A combined Pb-Hf-Nd isotope approach, *Earth Planet. Sci. Lett.*, *222*, 259–273.

Vlastélic, I., W. Abouchami, S. J. G. Galer, A. W. Hofmann, and C. Claude-Ivanaj (2001), Geographic control on Pb isotopic distribution and sources in Indian Ocean Fe-Mn deposits, *Geochim. Cosmochim. Acta*, *65*, 4303–4319.

Volkening, J., T. Walczyk, and K. G. Heumann (1991), Osmium isotope ratio determinations by negative thermal ionization mass-spectrometry, *Int. J. Mass Spectrom.*, *105*, 147–159.

von Blanckenburg, F., and T. F. Nägler (2001), Weathering versus circulation-controlled changes in radiogenic isotope tracer composition of the Labrador Sea and Northern Atlantic Deep Water, *Paleoceanography*, *16*, 424–434.

von Blanckenburg, F., R. K. O'Nions, N. S. Belshaw, A. Gibb, and J. R. Hein (1996a), Global distribution of beryllium isotopes in deep ocean water as derived from Fe-Mn crusts, *Earth Planet. Sci. Lett.*, *141*, 213–226.

von Blanckenburg, F., R. K. O'Nions, and J. R. Hein (1996b), Distribution and sources of pre-anthropogenic lead isotopes in deep ocean water from Fe-Mn crusts, *Geochim. Cosmochim. Acta*, *60*, 4957–4963.

von Damm, K. L. (1995), Controls on the chemistry and temporal variability of seafloor hydrothermal fluids, in *Seafloor Hydrothermal Systems: Physical, Chemical, Biological, and Geological Interactions*, *Geophys. Monogr. Ser.*, vol. 91, edited by S. E. Humphris et al., pp. 222–247, AGU, Washington, D. C.

von Damm, K. L., J. M. Edmond, B. Grant, C. I. Measures, B. Walden, and R. F. Weiss (1985), Chemistry of submarine hydrothermal solutions at 21°N, East Pacific Rise, *Earth Planet. Sci. Lett.*, *49*, 2197–2220.

Westercamp, D. (1988), Magma generation in the Lesser Antilles: Geological constraints, *Tectonophysics*, *149*, 145–163.

White, W. M., and B. Dupré (1986), Sediment subduction and magma genesis in the lesser Antilles: Isotopic and trace-element constraints, *J. Geophys. Res.*, *91*, 5927–5941.

White, W. M., and P. J. Patchett (1984), Hf-Nd-Sr isotopes and incompatible element abundances in island arcs: Implications for magma genesis and crust mantle evolution, *Earth Planet. Sci. Lett.*, *67*, 167–185.

White, W. M., B. Dupré, and P. Vidal (1985), Isotope and trace element geochemistry of sediments from the Barbados Ridge-Demerara Plain region, Atlantic Ocean, *Geochim. Cosmochim. Acta*, *49*, 1875–1886.

Whiteley, N. (2000), Investigation of palaeo-circulation in the southern Atlantic, southern, and northern Indian oceans over the last 14 Ma using hydrogenetic ferromanganese crusts, Ph.D. thesis, Univ. of Oxford, Oxford, U. K.

Woodhead, J. D., J. M. Hergt, J. P. Davidson, and S. M. Eggins (2001), Hafnium isotope evidence for ''conservative'' element mobility during subduction zone processes, *Earth Planet. Sci. Lett.*, *192*, 331–346.

Woodland, S. J., D. G. Pearson, and M. F. Thirlwall (2002), A platinum group element and Re-Os isotope investigation of siderophile element recycling in subduction zones: Comparison of Grenada, Lesser Antilles Arc, and the Izu-Bonin Arc, *J. Petrol.*, *43*, 171–198.

Zierenberg, R. A., P. Schiffman, I. R. Jonasson, R. Tosdal, W. Pickthorn, and J. McClain (1995), Alteration of basalt hyaloclastite at off-axis Sea Cliff hydrothermal field, Gorda Ridge, *Chem. Geol.*, *126*, 77–99.